

STUDY OF A COLD START FUEL PRODUCED BY AN
ACTIVE VAPOR UTILIZATION SYSTEM FOR
USE IN GASOLINE POWERED VEHICLES

by

JOHN CRAWFORD

A THESIS

Submitted in partial fulfillment of the requirements
for the degree of Master of Science in the
Department of Mechanical Engineering
in the Graduate School of
The University of Alabama

TUSCALOOSA, ALABAMA

2009

Submitted by John Crawford in partial fulfillment of the requirements for the degree of Master of Science specializing in Mechanical Engineering.

Accepted on behalf of the Faculty of the Graduate School by the thesis committee:

Marcus D. Ashford, Ph.D.
Chairperson

Paulius V. Puzinauskas, Ph.D.

Stephen M.C. Ritchie, Ph.D.

Robert P. Taylor, Ph.D.
Department Chairperson

Date

David A. Francko, Ph.D.
Dean of the Graduate School

Date

DEDICATION

This work is dedicated to the continuous pursuit of Knowledge and Achievement (KA) and those who believe in this journey.

LIST OF ABBREVIATIONS

ϕ_i	Volumetric fraction of species i
AIME	Alabama Innovation and Mentoring of Entrepreneurs
AQI	Air Quality Index
AFR	Air Fuel Ratio
ASTM	American Society for Testing and Materials
AVUS	Active Vapor Utilization System
C _n	Hydrocarbon with n of carbon atoms
E	Energy
E85	85% Ethanol mixed with 15% gasoline
EPA	Environmental Protection Agency
F_i	Moles of feed of species i
$F_{s,i}$	Moles of feed of separator species i
FTP	Federal Test Procedure
GC	Gas Chromatography
h	Planck's constant
L_{i-1}	Previous iteration's number of liquid moles
$L_{s,i-1}$	Previous separator iteration's number of liquid moles
HC	Hydrocarbon
HPLC	High-Performance Liquid Chromatography
N	Total number of pure species within the mixture
NAAQS	National Ambient Air Quality Standards

n_D	Refractive index of the mixture
n_{Di}	Refractive index of the species i
MTBE	Methyl Tertiary Butyl Ether
OBDS	On-Board Distillation System
PCM	Phase Change Material
PZEV	Partial Zero Emissions Vehicle
SIP	State Implementation Plan
T_A	Temperature of species A
TESD	Thermal Energy Storage Device
TESS	Thermal Energy Storage System
V	Total volume
VCSS	Vapor Cold Start System
V_i	Volume of species i
V_{i-1}	Previous iteration's number of liquid vapors
$V_{s,i-1}$	Previous separator iteration's number of vapor moles
x_i	Mole fraction of species i

ACKNOWLEDGMENTS

First I would like to thank God for the continuous and powerful gift of knowledge and understanding.

I would like to secondly thank my parents who always encourage my pursuit of excellence while never making me feel as if perfection was demanded. Their love support is greatly appreciated.

I would also like to thank Dr. Midkiff and Dr. Todd who made my presence at the University possible. I remember my interview as a senior in high school. They made me feel comfortable and welcome, even though I was under the weather. I thank them for that.

I also thank Dr. Marcus Ashford who recruited me into the graduate school program and helped guide me through academia as a mentor, friend and academic advisor. I thank him for that.

I would like to thank additional members of the UA faculty who helped in the creation of this thesis. Dr. Puzinauskas, committee member who taught various ME graduate classes and guided research in the realm of automotive engines. Dr. Richie, committee member who initially educated me in the art of separations. Dr. Daly and Dr. Spears, who advised and taught various analysis techniques that I used in the AIME center.

Finally, I would like to thank Mike Alff, upon whose research this work is based.

TABLE OF CONTENTS

DEDICATION	iii
LIST OF ABBREVIATIONS.....	iv
ACKNOWLEDGMENTS	vi
TABLE OF CONTENTS.....	vii
LIST OF TABLES	x
LIST OF FIGURES	xi
ABSTRACT.....	xiii
Chapter 1 INTRODUCTION.....	1
Background.....	1
Cold Starts.....	5
Evaporative Emissions.....	13
Current Research.....	15
Present Study	16
Motivation of Present Study	17
Organization of Thesis.....	17
Chapter 2 THEORY OF OPERATION	19
Introduction.....	19
Distillation	19
Natural Vehicle Distillation	21
Ideal AVUS Operation.....	22
Vapor Generation and Compressor Operation.....	23

Air/Fuel Separation and Condensate Storage	24
Fuel Delivery	25
Safety Considerations	25
Chapter 3 CONCEPT VALIDATION	27
Introduction.....	27
Gasoline and Gasoline Vapor Composition.....	27
Major Component Fuel	30
Chapter 4 EXPERIMENTAL SETUP	34
Introduction.....	34
AVUS Experimental Apparatus.....	34
AVUS Preparation	38
AVUS Operation.....	39
E85 AVUS Operation	41
Chapter 5 TESTING, RESULTS AND DISCUSSION.....	42
Introduction.....	42
Temperature and Pressure Profiles	43
Temperature	43
Pressure	45
Refraction Results Testing and Results	47
Ethanol Blends	50
AVUS Condensate	52
Infrared Testing and Results.....	53

Phase Separation	56
Infrared.....	58
Chemical Analysis Testing and Results.....	65
Chapter 6 AVUS COMPUTER MODEL.....	78
Introduction.....	78
Assumptions.....	78
Fuel Tank	80
Fuel Tank Model Results	82
Separator	85
Separator Model Results	87
Separator Temperature Correction and Results	89
AVUS Model Considerations	92
Chapter 7 CONCLUSIONS AND RECOMMENDATIONS.....	93
Introduction.....	93
Conclusions.....	93
Recommendations.....	95
REFERENCES	96
Appendix A: Data Results from Parent Fuels and AVUS Samples.....	99

LIST OF TABLES

Table 1. Comparisons of Major Component Fuels by Carbon Number (Santoso, 2002; Senda, 2000; & Na, 2004).....	32
Table 2. Average temperatures and pressures.....	47
Table 3. Measured and accepted index of refraction values.....	49
Table 4. Refractive index for name brand gasoline.....	51
Table 5. Index of refraction for AVUS samples.....	52
Table 6. Ethanol content based on infrared transmittance equations.....	64
Table 7. Hydrocarbon composition of AVUS samples.....	67
Table 8. Assumed hydrocarbon composition of AVUS samples.....	71
Table 9. Drivability index of AVUS samples from MDA fuel.....	74
Table 10. Drivability index for AVUS samples from E85-MDA fuel.....	75
Table 11. Condensate and residual volumes collected.....	77
Table 13. Properties of MDA fuel component species at 25 °C and 100 kPa.....	80
Table 14. Original MDA fuel composition.....	82
Table 15. Initial and final moles of MDA fuel components in computer model.....	83
Table 16. Model composition of both the residual fuel and the condensate fuel.....	88
Table 17. Final composition of both the residual fuel and the condensate fuel with temperature correction.....	91
Table 18. Comparison of model and actual AVUS results.....	91

LIST OF FIGURES

Figure 1. Carbon canister operation.....	14
Figure 2. Sample apparatus for simple distillation	20
Figure 3. Proposed in vehicle AVUS operation.....	22
Figure 4. Carbon number breakdown of pump gasoline and AVUS condensate (Alff, 2007).....	28
Figure 5. Comparison of compositions of pump gasoline and gasoline vapors (Na <i>et al</i> , 2004).....	29
Figure 6. Experimental setup of the AVUS	37
Figure 7. Fuel temperature profile as seen by during SHED testing (El-Sharkawy, 1998).	40
Figure 8. Fuel temperature profiles from AVUS experiments on MDA fuel.....	44
Figure 9. Fuel temperature profiles from AVUS experiments on MDAE85 fuel	44
Figure 10. Fuel tank and separator pressure profiles	45
Figure 11. Refractive index and variation of deviation for MDA-ethanol fuels	51
Figure 12. Infrared absorption for alcohol and non-alcohol fuels	55
Figure 13. Percent ethanol rich phase in ethanol mixtures.....	58
Figure 14. Infrared absorption for ethanol mixtures.....	59
Figure 15. Infrared absorption for ethanol mixtures for OH and CO bonds.....	60
Figure 16. Infrared transmittance for ethanol mixtures	61
Figure 17. Ethanol content based on Infrared absorption.....	62
Figure 18. Infrared absorption for AVUS condensates	64
Figure 19. Assumed hydrocarbon composition of AVUS samples from MDA fuel.....	72

Figure 20. Assumed hydrocarbon composition of AVUS samples from E85-MDA fuel	72
Figure 21. Distillation curves for AVUS samples from MDA fuel	73
Figure 22. Distillation curves for AVUS samples from E85-MDA fuel	75
Figure 23. Sample output from NIST FLASH routine	82
Figure 24. Initial fuel composition by mole percent.....	83
Figure 25. Initial and final fuel composition by mole percent.....	84
Figure 26. Change in fuel tank temperature and mole percentages	85
Figure 27. Total composition of the removed fuel tank vapors	85
Figure 28. AVUS model condensate composition.....	88
Figure 29. AVUS condensate composition with temperature correction	90

ABSTRACT

This research focuses on the continuous development of the Active Vapor Recovery System (AVUS) which has the potential to reduce unburned hydrocarbon emissions from automobiles. The AVUS collects, condenses and stores hydrocarbon vapors from the fuel tank and saves them in a pressurized storage tank for later use as a cold starting fuel. This highly volatile starting fuel has the capability to reduce tailpipe emissions that occur during cold starts, as well as evaporative emissions that occur while the vehicle is at rest.

Instead of commercial gasoline, the bench top AVUS was run using a five component fuel composed of 25% iso-pentane, 17.5% hexane, 17.5% heptanes, 17.5% toluene, and 22.5% isooctane; as well as an E85 mixture composed of 15% five component fuel and 85% ethanol. The condensate produced from AVUS was then analyzed using simple gas chromatograph techniques and found to have as much as 75% iso-pentane. Such a mixture would be an excellent starting fuel. Successive tests on the same batch of fuel proved that AVUS can produce this starting fuel without depleting the parent fuel of the species needed for non-AVUS starts.

Index of refraction and infrared tests were also used in an attempt to establish reliable correlations between the condensate composition, refractive index, and infrared absorption that could be used for onboard analysis of the starting fuel. However, index of refraction results were found to be inconclusive while infrared testing proved to have great potential for determining alcohol concentration.

Chapter 1 INTRODUCTION

Background

Even though the average cost of a gallon of gasoline has dropped significantly since its peak in the summer of 2008, gasoline consumption is still a major part of most families budgets, especially in trying economic times. Surprisingly, after adjusting for inflation and the rise in per capita income over the last decade, the American public only pays about 1.3 times more than they did in 1998 (Taylor, 2006). With the expected decline in the production of crude oil, a rise in the cost of gasoline will follow and automobiles should ideally use every ounce of fuel that poured out of consumers' pockets and into gas tanks. However, they do not. In fact, modern vehicles emit unburned hydrocarbons, wasted components of valuable gasoline, every second they run. Aside from a wasteful byproduct of automobile combustion, hydrocarbon emissions also cause adverse health effects and aid in the formation of smog and emissions that have been a problem since Ford produced the first Model T in 1903. However, since then the U.S. government has implemented emissions regulations and standards to curb the unnecessary production of hydrocarbons.

Hydrocarbons are emitted from the incomplete of burning of organic compounds such as oil, wood, and rubber, and can be composed completely of hydrogen and carbon (South Coast AQMD). However, automobile hydrocarbon emissions can be largely grouped into two types and all come from gasoline, which is a complex mixture of

hundreds of hydrocarbons of various sizes and shapes. The first type, tailpipe emissions, is created from the incomplete combustion of the larger hydrocarbons in gasoline. This actually occurs in the automobile engine and the majority of these emissions occur within the first 90 seconds after the automobile has been started. These emissions are mostly due to the low volatility of fuel at lower temperatures, and the over fueling that occurs in the combustion chamber to compensate. The second type, evaporative emissions, occurs when unburned fuel is heated in the fuel system, vaporizes, and escapes from the car. Once these dangerous chemicals are released into the atmosphere, hydrocarbons can interfere with a person's oxygen intake by reducing the amount of available oxygen through displacement.

Furthermore, hydrocarbons aid in the formation of ozone, a highly reactive bluish colored oxidizing gas that breaks-down organic materials. The hydrocarbons react with nitrogen oxides in the presence of sunlight and produce the toxic compound. In the ozone layer, a region of the stratosphere located between about 10 km and 50 km above the surface, helpful ozone blocks photons with shorter wavelengths of ultraviolet light from the Sun that would be harmful to most forms of life in large doses (South Coast AQMD). In this way ozone protects life on Earth. Although the ozone layer protects earth from harmful rays in the atmosphere, on the surface it can cause many health problems. Ozone is a component of smog, the smoky dark cloud that covers many of the more populous and industrialized cities of the world. The term smog is a very broad term that can refer to any of the many different forms of particulate matter that cause air pollution and the intensity of smog in an area is usually determined by measuring ground level of ozone in that area (Brochert, 2000). However, human symptoms such as coughing, shortness of

breath, wheezing, fatigue, throat dryness, chest pain, headache and nausea can be signs of ground level ozone exposure. Other respiratory problems such as inflammation of lung tissue, reduced lung capacity, asthma, lung cancer, and accelerated lung aging can all be linked back to ozone exposure as well (South Coast AQMD). Unfortunately, these adverse health effects are more intense for those with pre-existing health problems, such as asthma. For example, scientific studies have shown that the number of lung infections, hospital visits and hospitalizations goes up with increasing smog levels in those with asthma or other lung conditions (Brochert, 2000). Other groups at high risk from ozone exposure include children, athletes, and senior citizens. Most believe that long term exposure to ozone can cause permanent damage and reduce the ability of the respiratory system to fight infection and remove foreign particles such as particulate matter. However, the effects of short term exposure can be reversed by being removed from a ground level ozone environment (South Coast AQMD).

Due to previously mentioned health concerns and others caused by pollution of the air, land, and water, the United States government have established the Environmental Protection Agency (EPA) to “protect human health and to safeguard the natural environment—air, water, and land—upon which life depends.” Since its creation in 1970, the EPA has written and enforced regulations that parallel environmental legislation written by Congress (History). The most recent automobile regulation comes in the form of the Tier 2 Vehicle and Gasoline Sulfur Program. Some of the key points of this program are that all passenger vehicles are subject to the same emission standards, gasoline must now have low sulfur content, and standards apply to all light vehicles regardless of fuel - including gasoline, diesel and alternative fuels (Tier 2).

While emission standards regulate automobiles, the EPA has also put into place the National Ambient Air Quality Standards (NAAQS) which monitor the concentration of six major pollutants as they pertain to public health and the environment. The regulated pollutants are carbon monoxide, lead, nitrogen dioxide, particulate matter (PM10 & PM2.5), ozone, and sulfur dioxide (Technology Transfer). These compounds are measured and reported using the Air Quality Index (AQI), which is a 0-500 scorecard used to classify and categorize geographic areas of high pollution. In general, values fewer than 100 are satisfactory, 101-150 are dangerous for those sensitive groups mentioned earlier, and over 151 is unhealthy to the general public (Air Quality).

Within the U.S., counties whose air pollution levels persistently exceed the national ambient air quality standards may be designated "nonattainment" by the NAAQS. States with nonattainment areas within their borders must compose a State Implementation Plan (SIP) which details the processes that will be taken to improve the air quality in nonattainment areas. When a nonattainment area meets the standards and additional re-designation criteria, the EPA will designate the area as a "maintenance area." By definition a maintenance area is a geographic area that had a history of nonattainment, but is now consistently meeting the NAAQS (Technology Transfer). Typically nonattainment counties will carry gasoline with up to 10% ethanol by content. This gasoline additive helps to reduce emissions.

These exceedingly strict government regulations have forced car manufacturer to create advances in the reduction of automobile emissions over the years. The original EPA regulations indirectly produced such inventions as the catalytic converter which is still used to oxidize unwanted hydrocarbon compounds from tailpipe emissions into

water and carbon dioxide; while more recent requirements have seen the implementation of carbon canisters which helps curb evaporative emissions. These original devices and their upgrades were directly designed to attack the two major sources of automobile hydrocarbon emissions – tailpipe and evaporative, but more can be done. Studies have shown that up to 95% of tailpipe hydrocarbon emissions occur within the first 60-90 seconds after starting a cold engine. This time period is referred to as the cold start period (Ashford & Matthews, 2005). Other studies have shown that evaporative emissions from the fuel tank and engine, which can occur during refueling, operation, and while the vehicle is at rest, can produce several times tailpipe hydrocarbon emissions (Lyons, 2000). One could reasonably assume that by reducing or eliminating cold start and evaporative emissions, total hydrocarbon emissions can be significantly decreased; therefore there have been numerous research studies and inventions targeted at doing just that.

Cold Starts

The high emissions regularly experienced during cold start are due primarily to two reasons: low fuel volatility and poor catalytic converter performance. At 20 °C only 10-30% of gasoline actually vaporizes when injected into the combustion chamber. That means 70-90% of the fuel remains in the liquid phase. Therefore the engine must inject additional fuel to compensate for the low volatility. Typically this over compensation can be from 8-15 times the stoichiometric amount in order to produce enough vapors for reliable ignition. The non-vaporized fuel remains as a liquid till combustion. The fuel vapors are ignited by the spark plug and most of the liquid fuel vaporizes and exits the

engine as unburned hydrocarbons. Overall this results in very rich air/fuel ratios that only partially combust (Ashford, 2006).

However, under ideal conditions the catalytic converter would eliminate many of the unburned hydrocarbons by reduction and oxidation, but during this cold start period a standard three-way convertor will not reach its “light off” (meaning a 50% hydrocarbon conversion rate) temperature until 30-40 seconds after the start during the FTP drive cycle. Unfortunately and ironically, the catalyst is the least efficient when it is most needed during the operation of the vehicle. The result of this combination of less than ideal circumstances is high tailpipe hydrocarbon emissions (Ashford, 2006)

Many researchers and inventors have focused on correcting these problems and reducing hydrocarbon emissions during cold starts. Most of these projects have fallen into two categories: improving engine starting parameters and improving catalytic convertor performance. Recently there has been more work in a third category where researchers use an alternative starting fuel in the engine during cold starts to reduce emissions. While the other two categories attack the symptoms of the problem, this approach actually deals with the low volatility of the fuel, the true cause of the problem

Various attempts have been made with starting parameters to reduce cold start emissions. One of the most common is the lean start strategy which increases the chance that all of the fuel will be burned. Gong Li (2006) claimed that the first firing cycle was extremely important for cold start emissions. These researchers found that by improving the combustion in the first cycle, high cylinder temperatures could be reached sooner. This scenario is favorable for combustion in the following cycles, therefore leading to lower emissions. Li sought to achieve this by changing the amount of excess air and the

spark angle. It was found that for a 125 cm³, four-stroke, air cooled, spark-ignited engine with a single port injector running on liquefied petroleum gas, hydrocarbon emissions could be reduced by advancing the spark timing. Hydrocarbon emissions also reached a minimum for an optimal excess air factor of 0.53. Decreasing past 0.53 resulted in higher emissions (Li, 2006). It is reasonable to assume that similar results would be achieved in a gasoline engine.

Although this and other comparable lean strategies can reduce cold start emissions, these methods also have greater chance of poor starts and misfires. These calibrations must also take into account the lean limit for various fuels which further complicates the strategies. The more volatile the fuel, the leaner it can be started; resulting in reduced emissions. However, the lower volatile fuels are prone to re-condense on cool engine components (Alff, 2007), and an initial misfire results in even more hydrocarbons emissions and impacts the stability and emissions of later cycles (Li, 2006). Lean strategies can definitely aid in cold start emissions, but a more reliable and stable solution is needed.

Another method of reducing emissions by varying starting parameters has been to actually increase the starting temperature of the engine by means of pre-heating the combustion chamber. Gumus (2008) designed and tested a thermal energy storage system (TESS) that uses a thermal energy storage device (TESD) to pre-heat the engine for 500 seconds before cold starts. The TESD supplies energy to the engine by the rejection of heat during the phase change of a heat storage material. The energy source was able to raise the average temperature of the engine block from 2 to 20.6 °C in about 1000 seconds; furthermore, an engine temperature of about 17.4 °C was reached in just over 8

minutes. Results of the study show that CO and hydrocarbon emissions decreased by 64% and 15%, respectively, during the first 200 seconds of operation. $\text{Na}_2\text{SO}_4 \cdot 10\text{H}_2\text{O}$, which is inexpensive and abundant, was used as the phase change material (PCM) of the TESD. During the drive cycle, the PCM recovers energy from the engine coolant to return to the liquid phase for the next cold start. A disadvantage of this system is that it works best within a 12 hour waiting duration. After this point the heating effect of the TESD begins to decrease (Gumus, 2008). Tests would also need to be done on the repeatability of the PCM to determine at what intervals, if any, that the PCM would need to be changed.

Instead of trying to reduce the amount of hydrocarbons produced by the engine, other researchers and inventors have focused on eliminating the hydrocarbons by means of the catalytic convertor. Some of the more common ways of improving performance are by preheating the catalyst, either electrically or chemically, or the precatalyst method. While preheating is self-explanatory, the precatalyst method uses a second smaller convertor which is located as close as possible to the cylinder head. This location takes advantage of exhaust heat to improve performance of the precatalyst. Both these methods aim to decrease the time it takes the catalyst to become active or light off, the point at which the convertor achieves 50% efficiency. Karkanis (2004) suggested and tested a novel idea to limit the exposed surface area of the catalyst during the start to decrease the time to catalyst light off. He reasoned that the surface area of the catalytic convertor is optimal for the volume of exhaust gases emitted from the engine at wide open throttle, and at any other load, less surface area is actually needed. Therefore, by reducing the

active surface area of the catalyst during cold starts, Karkanis was able to reduce the light off time and decrease hydrocarbons (Karkanis, 2004).

Karkanis's study found that for his test engine idle conditions the optimal exposed surface area of the catalytic converter is 20%, which lead to a decrease in the light off period from 240 seconds to 134 seconds and a reduction in hydrocarbon emissions by 20%. In order for this system to be used in practice, automakers would need to design a mechanism to actively change the used catalyst surface area based on the volume of exhaust gases from the engine. This volume is related to the engine's rpm's and load. This automated catalyst would in effect make the catalytic convertor an actively responsive part of the engine (Karkanis, 2004)

Ramanathan and his team of researchers were able to achieve better catalyst performance without pre-heating the catalyst. They found that by varying the catalyst loading, the catalyst distribution along the channel length and the average thickness of the catalyst wash, hydrocarbon emissions could be reduced. When compared to a standard uniformly loaded catalyst, two-zone catalyst distribution with more catalyst near the inlet reduced the cumulative emissions substantially. Furthermore, Ramanathan discovered that there is an optimal washcoat thickness and/or catalyst loading beyond which the performance of the converter does not improve substantially. By adjusting these variables, reduction of light off time of the catalyst was achieved without actively pre-heating the catalyst or changing the performance of the engine (Ramanathan, 2004). Coupling this technique with either of the other methods for improving cold start emissions with further reduce the light off time and cumulative cold start emissions.

More recently researchers have focused on alternative cold starting fuels. In 2003 Ashford and Matthews created and tested the On-Board Distillation System (OBDS) which produced a highly volatile starting fuel which resulted in improved air/fuel mixtures that are not possible with commercial grade gasoline at any engine temperature. Ashford's apparatus utilizes the heat from the engine coolant system to distill consumer grade gasoline and store the more volatile species in a low pressure tank for cold starts. The heavier components are sent to the engine for normal operation. The distillate stored in the low pressure tank was fed to the fuel rail during cold starts to achieve lower initial hydrocarbon emissions. Once the engine had reached a suitable temperature, the fuel source was switched from the distillate to the surrogate tank gasoline (Ashford & Matthews, 2003).

Ashford installed the OBDS on a 2001 Lincoln Navigator with the engine starting calibration modified to a lean strategy. Results showed a 70% reduction in CO tailpipe emissions, and an 81% reduction in hydrocarbon tailpipe emissions. The OBDS also had the effect of reducing catalyst light off time by 57% and increasing fuel economy by 1% on the FTP drive cycle. By using a more volatile starting fuel, the OBDS can decrease or eliminate fuel mixture enrichment, a major source of cold start emissions. The volatility of the distillate fuel is function of the composition of the parent fuel, but adjustment of OBDS parameters and calibrations could make the gasoline distillate less dependent on the parent fuel volatility (Ashford & Matthews, 2003). However, the very nature of the OBDS has drawbacks. By removing the light hydrocarbons from the gasoline, the residual fuel is less volatile which could eventually cause problems after multiple distillations of the parent fuel. Furthermore, the volatile fuel produced by the OBDS has

an increased vapor pressure at temperatures usually seen by the fuel tank. This increased volatility of the starting fuel may lead to increased evaporative emissions.

Other attempts to collect light hydrocarbons have been investigated as well. In 2004, Reddy designed and patented a fuel system that is based on the principle that low pressure areas in the fuel lines encourage fuel vaporization. It incorporates an active vapor generator that separates the liquid gasoline from the vapor and pumps the volatile vapors to a secondary carbon canister. The vapor generator runs and collects vapors until the secondary canister reaches a predetermined situation point, and then the vapors are stored until the next cold start. A downside to this approach is that fuel vapor, not a liquid, is used during the cold start. Ambient air is pumped through the canister and into the engines air intake. Fuel air mixture is estimated by use of flow and oxygen sensors, but the exact AFR of a pre-mixed vapor is hard to determine quickly and inexpensively. Furthermore, determining the quality and quantity of fuel in the canister could prove difficult and result in misfires and greater hydrocarbon emissions. Unfortunately no quantitative data is available for the actual hydrocarbon emissions for this system (Reddy, 2004).

Servati and Marshall designed a Vapor Cold Start System (VCSS) similar to Reddy's cold start canister system except with one major difference: instead of further encouraging the production of vapors, Servati used the existing carbon canister as the vapor source. The canister typically stores evaporated hydrocarbons for use during normal engine operation. By incorporating a hydrocarbon sensor and an air/fuel premixing chamber, Servati was able to produce an AFR mixture suitable for cold starts. Contrary to normal engine operation, the intake air is disconnected during cold starts so

that a separate dilution chamber can add air to the fuel mixture and send to the engine (Servati, 2005).

Servati tested the VCSS using a 4.6 L F150 V8 Ford Truck. The vehicle was equipped with a fully charged 5 L carbon canister, an on board hydrocarbon sensor, and a specially designed vapor delivery manifold. Results from the study showed that the VCSS was capable of cold starting and providing extended idle for the engine, as well as over 70% reduction in emissions when compared to normal fuel injection starts. However, the method by which the vapors are removed from the canister and the unknown variable of the quantity of vapor in the canister may lead to problems with consistent and reliable starts. The system creates a suitable AFR in the mixing chamber but if there is no vapor in the canister, starting will be impossible. Prolonged starting times are also experienced due to the canister purge (Servati, 2005).

Most recently at the University of Alabama, Ashford and Alff designed a bench top Active Vapor Utilization System (AVUS). Unlike the work of Reddy and Servati, AVUS actively collects vapor naturally produced in the fuel tank during normal operation and diurnal temperature swings and returns the vapor to a liquid form for engine operation. Liquid fuel solves a major problem of the Reddy and Servati systems, unknown AFR. Once removed from the fuel tank, the vapors are compressed, cooled, and stored in a pressurized tank for use in cold starting. Unfortunately, in Alff's study the AVUS condensate was unable to be tested in a vehicle and the industry standard ASTM D86 Distillation test was unsuitable for testing due to the highly volatile nature of the condensate. However, a simple evaporation test showed that the AVUS condensate

vaporizes at a rate nearly twice that of iso-pentane (Alff, 2007). The work presented here looks to further investigate the practicality of the AVUS.

While these inventions have the potential to allow the gasoline engine to continue to make cleaner power, many automobile makers are looking into alternative fuels as ways to solve the emissions problems. Hydrogen, bio-diesel, electricity, and natural gas are all possible energy sources for automobiles, but ethanol is one of the more plausible and readily available alternatives that can be used today. In fact, thousands of vehicles currently on the road are capable of functioning on ethanol mixtures as high as 85% ethanol by volume. However, ethanol is much less volatile than commercial gasoline and would lead to additional cold start problems. The use of AVUS on an E85 blend will also be investigated.

Evaporative Emissions

A conservative estimate predicts that evaporate hydrocarbon emissions can be as high as three to four times that of tailpipe hydrocarbon emissions (Lyons, 2000). Generally, evaporative emissions can be classified into two types: refueling losses and fuel system losses. Refueling losses occur when vapors escape from the gasoline tank when the cap is removed and fuel is pumped during refueling. The liquid gasoline displaces the vapors within the tank, and the vapors escape to the atmosphere. Estimates show that in 1999 refueling losses were responsible for 22,000-88,000 tons of hazardous air pollutants and 470,000 tons of VOC's. For these reasons, states are requiring the use of vapor recovery devices are refueling stations. Estimates show that these systems will save up to 284 millions liters of gasoline from 1998-2020 (Commonly Asked, 2006).

Current vehicles attempt to limit evaporative emissions from the fuel tank by use of a carbon canister filled with an activated charcoal adsorbent as depicted in Figure 1. In most cases the fuel vapors are fed to the canister when a threshold pressure limit is reached in the fuel tank. This may occur at anytime, including while the vehicle is running. During engine operation, the vapors are released from the carbon canister and pulled into the intake manifold along with ambient air. Then these vapors are burned in the combustion chamber along with injected fuel. However, the carbon canister has disadvantages as well. If the canister becomes saturated while the engine is not running vapors are released to the atmosphere and therefore increase emissions. It is also possible that under heavy operating conditions the rate of vapor generation may exceed the adsorption capabilities of the carbon canister and lead to atmospheric release of hydrocarbons.

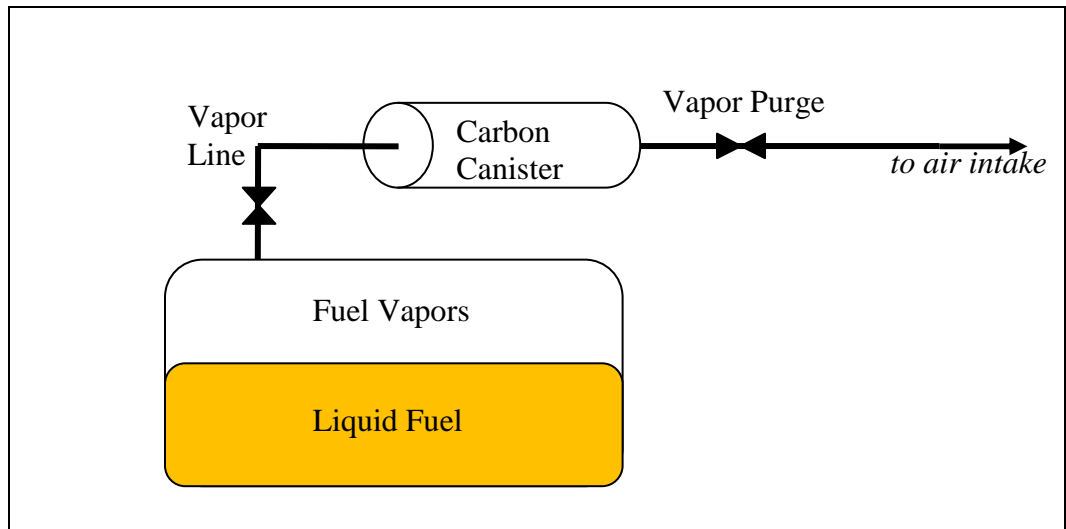


Figure 1. Carbon canister operation

In addition to the work mentioned previously by Reddy and Servati, research has been done to supplement and replace the standard carbon canister. The added benefit of the previously stated works is that those systems use the vapors for cold starts and not

just for normal operation (Lebowitz & Levette, 2005). Alff mentions that PZEV canisters containing high capacity pellet, activated carbon coated ceramics, and activated carbon coated foams may be promising depending on the designer's specifications (Alff, 2007)

The second type of evaporative losses can be further broken down into three types:

- Diurnal: evaporative emissions from generated by the daily ambient temperature changes
- Hot soak: gasoline vapors generated following engine shutdown, due to vaporization of the remaining fuel under the hood
- Running losses: vaporized gasoline due to the hot engine, pavement, and exhaust system when the car is running.

Aside from the vapors generated in the fuel tank from these sources, the remaining evaporative losses occur in or near the engine. Researchers have found that significant amounts of evaporative emissions occur from vehicle intake air manifolds, fuel injectors, and other fuel delivery components. Work has been done to limit these emissions using activated carbon hydrocarbon filters and specially designed injectors; however, engine evaporative emissions are beyond the scope of this work.

Current Research

A 2004 South Korean study done on a mixture of five major gasoline brands determined that their composition contained only 55%, 48%, and 52% C₂-C₆ by weight for winter, spring, and summer gasoline blends respectively where the notation C_n refers to a hydrocarbon molecule with n carbons. However, at 0, 11, and 24 °C the vapor above gasoline contains 98%, 96%, and 95% C₂-C₆ respectively (Na, 2004), and at higher

temperatures the composition would shift allowing for heavier hydrocarbons. Researchers have already proven that a starting fuel composed of highly volatile hydrocarbon species can reduce both hydrocarbon and CO tailpipe emissions, as well as reduce catalyst light off times by as much as 50%. A simple but novel solution exists. These naturally occurring gasoline vapors should be collected, condensed, and stored for use exclusively for cold starts. By using a liquid starting fuel, the unknown AFR problems of the Reddy and Servati systems are alleviated. Because significant amounts of hydrocarbon emissions occur in the first 90 seconds after starting the engine, a system that collects gasoline vapors for cold starts could lead to considerable reductions in both tailpipe and evaporative hydrocarbons emissions while improving the fuel economy of the vehicle.

Present Study

This study continues to examine the practicability of an Active Vapor Utilization System, AVUS, that collects, condenses, and stores vapors naturally produced on the vehicle during diurnal temperature swings, hot soaks, and normal operation. Today's vehicles do collect gasoline vapors in a carbon canister, and the vapors are used in the engine if they are not purged to the atmosphere because of canister saturation; however these vapors could be used more efficiently and result in lower emissions and better fuel economy. AVUS collects vapors for use in cold starting while the lightest non-condensable components of the gasoline are sent to the carbon canister for use during normal operation. While OBDS and Reddy's vapor generation system actively produce vapors from the commercial gasoline, AVUS only collects vapors that occur naturally in the fuel tank. The added benefit of AVUS is that it separates the lighter, highly volatile species from the other vapors and condenses the heavier components of the vapor into a

starting fuel. This allows for easier control of the AFR. In order to simplify composition analysis, the present study uses a major component fuel instead of commercial gasoline as seen in the previous AVUS experiments. Vapor composition, storage of fuel vapors, separation techniques, E85 vapor composition, and ethanol content measuring techniques will all be examined. A computer model based on the NIST SUPERTRAPP program is also compared actual results.

Motivation of Present Study

- To provide a system able to reduce tailpipe emissions in automobiles by producing a highly volatile starting fuel capable of near complete combustion during a cold start
- To provide an inexpensive alternative solution to cold start catalysts and large activated carbon canisters for the reduction of hydrocarbon emissions
- To reduce evaporative emissions produced by the gasoline tank by capturing, compressing, and storing vapors for later use
- To provide a cold start system capable of working on flex-fuel engines that run on E85
- To determine the feasibility of refractive index and infrared adsorption as onboard methods of determining ethanol content in gasoline and starting fuels

Organization of Thesis

This thesis is divided into seven chapters. The current chapter introduced the motivation behind AVUS and other research that has been done in the area of reducing hydrocarbon emissions. The following chapter outlines the AVUS theory of operation which is based on simple distillation. The chapter then discusses AVUS operation and its

probable interaction with actual vehicle components. Chapter 3 aims to validate the AVUS concept while Chapter 4 details the AVUS experimental setup and laboratory operation. The tests that were performed on the AVUS starting fuel and the results of those tests are presented and discussed in Chapter 5. The testing techniques for AVUS condensate include refractive index, infrared absorption, and gas chromatography. The NIST based computer model and its results are discussed in Chapter 6. Finally, Chapter 7 outlines the conclusions of this study and presents recommendations for future work.

Chapter 2 THEORY OF OPERATION

Introduction

The purposes of this chapter are to discuss the basic principle behind AVUS operation, give detailed explanation as to the proposed operation of AVUS in a vehicle, and define AVUS operation.

Distillation

The basic underlining principle of AVUS is distillation, which has been used by man dating back to ancient Arab times when chemists used it to isolate perfumes. By definition, distillation is the method of heating an impure liquid until its vapor pressure equals that of the surroundings and begins to boil, then collecting and condensing the resulting vapors (Seader, 2008). In this way one is able to separate components of the liquid with varying boiling points. A species boiling point is the temperature at which the vapor pressure of the compound equals the external pressure at the surface of the liquid.

The simplest example of distillation is a liquid compound containing only two species, A and B, with drastically different boiling points, T_A and T_B , but equal concentrations. Assuming the mixture is placed in an apparatus similar to Figure 2, and that liquid A has a lower boiling point, the mixture will begin to boil near T_A . The resulting vapors are collected, cooled, and stored in a separate container. If kept at a temperature near T_A , the liquid remaining in the original flask will be high in concentration of liquid B, while the condensate will have a strong concentration of liquid

A. However, this is not a perfect process. The vaporization of liquid A, does cause small amounts of B to vaporize and be carried to the storage container. Multiple stages of distillation are needed if purification of compounds is required (Seader, 2008). Actually, distillation is the method by which the petroleum industry separates gasoline, kerosene, diesel, oil and natural gas from crude oil (Buell, 2003).

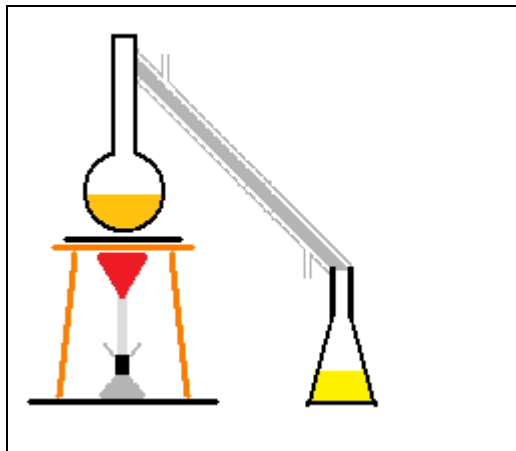


Figure 2. Sample apparatus for simple distillation

However, gasoline is not a simple mixture comprised of two liquids with drastically varying boiling points. In fact, commercial gasoline is a complex compound containing hundreds if not thousands of various hydrocarbons of different thermodynamic properties. Fortunately, the very composition of gasoline is an asset to the AVUS, which uses simple distillation to separate the lighter hydrocarbons, C₂-C₆, from the heavier species, C₇ and heavier. Simple distillation is a single stage process ideal for separating liquids whose boiling points vary by 50 degrees or more. This process will not separate single components from the parent mixture, but it will effectively remove groups of species with similar volatilities from the larger mixture. This is called the concept of relative volatility, a ratio comparison of the vapor pressures

of the components in a liquid mixture of chemicals. Mixtures with relative volatilities closer to one will be hard to separate, while those approaching zero or infinity will be easily separated (Seader, 2008). AVUS utilizes this type of distillation to separate light hydrocarbons from the heavier species.

Natural Vehicle Distillation

The vehicle fuel tank functions as the distillation column for the AVUS process. Unlike the OBDS, AVUS passively heats the fuel using the same sources that cause evaporative emissions: daily ambient temperature changes, hot pavement, the vehicle exhaust system and re-circulated fuel that has been heated by the engine when the car is running. As the heat from these sources warm the fuel tank and the gasoline, vapors form in the space above the gasoline. Because AVUS relies on external and inconsistent sources of heat for vaporization, the temperature used to distill the gasoline is not controlled and therefore the species that are captured are also not controlled. However, more volatile species vaporize faster and are more likely to be used by AVUS to produce a starting fuel. This process will be referred to as natural distillation as the heat comes from environmental sources.

Cold starts are a greater emission problem during cold months when fuel is even less likely to vaporize on engine components. One may think that AVUS would be impractical to use in colder temperatures due to its dependence on external heating; however, AVUS can take advantage of seasonal and regional fuel blending. In colder climates, fuels are blended with a higher concentration of volatile species which AVUS can capture for use in cold starts.

Ideal AVUS Operation

The AVUS has the ability to significantly reduce evaporative emissions from fuel tanks, and cold start emissions from gasoline vehicles. The system produces a highly volatile starting fuel from vapors obtained from the refueling process and the natural distillation that occurs in the fuel tank. These vapors, which would normally be directly into an activated carbon canister for later use during normal operation, are collected from the fuel tank by a compressor and sent to an air/fuel separator. Here AVUS uses the volatiles of the various hydrocarbon species of the gasoline vapor to divide non-condensables such as air and C₂ from other hydrocarbons that can be condensed. Separating the air from the fuel and re-condensing the vapors is a key advantage of AVUS in that it allows for a smaller storage volume, lower risk of ignition, and more control of the AFR ratio during the actual cold start. The remaining vapors are purged to a modified carbon canister while the condensed hydrocarbons are stored for later use. The condensed, highly volatile starting fuel can then be effectively used to start the vehicle. Ideally, the entire system is completely sealed to the atmosphere to prevent additional hydrocarbon emissions. Figure 3 depicts AVUS incorporation into existing fuel systems.

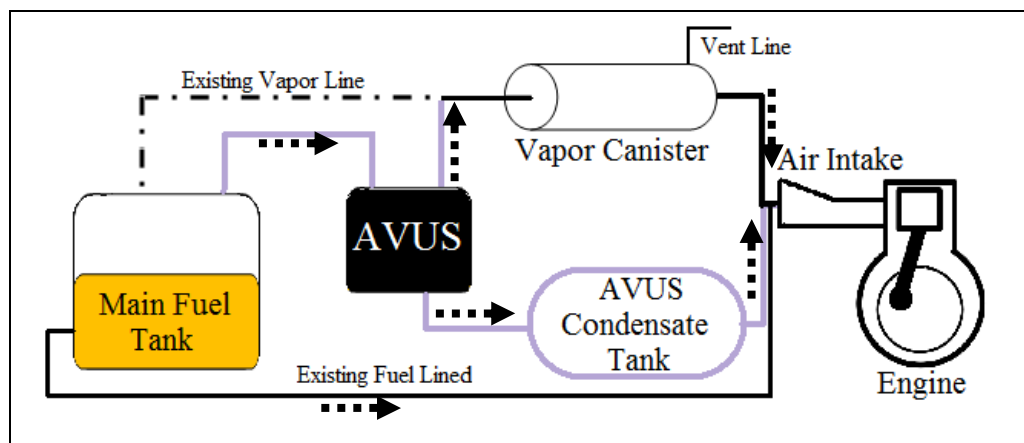


Figure 3. Proposed in vehicle AVUS operation

Vapor Generation and Compressor Operation

Daily ambient temperature changes, hot pavement, the vehicle exhaust system and re-circulated fuel that has been heated by the engine add heat to the vehicle fuel tank and cause a rise in fuel temperature, and therefore, vapor generation. There is always a mixture of vapor and air in the fuel tank, but more vapors form as the temperature increases. As the boiling temperature and vapor pressure of various components of the gasoline are reached, vapor generation causes a rise in the fuel tank pressure; a portion of the pressure is due to the volumetric expansion of the liquid fuel.

The fuel temperature and composition, as well as the pressure within the fuel tank, are factors that determine the vapor generation rate and composition. A fuel composed of more volatile species will quickly generate vapors at a lower temperature, while a less volatile fuel will be slower to generate vapors and will do so at higher temperatures. Aside from heat addition, refueling also causes the pressure within the fuel tank to increase. The liquid fuel displaces vapors already present within the fuel tank and causes the pressure to rise. The exact vapor rate is impossible to determine because of the amount of uncontrolled variables in the vehicle and the fuel.

Once vapor generation and/or vapor displacement causes the fuel tank pressure to reach a predetermined pressure limit, the compressor is activated and draws the vapor/air mixture from the fuel tank and concurrently relieves the pressure within the fuel tank. Once a predetermined lower limit is reached within the fuel tank the compressor deactivates and the process repeats as pressure rebuilds within the tank. Current vehicles use the carbon canister to handle vapor generation through passive capture; however, AVUS actively captures these vapors that are already produced within the fuel tank.

Many of the gasoline components that AVUS retrieves do not condense at atmospheric pressure unless the temperature of the vapors is lowered. For example, butane and iso-pentane, two of the most valuable vapors that AVUS recovers, will not condense until $-0.5\text{ }^{\circ}\text{C}$ and $28\text{ }^{\circ}\text{C}$ at atmospheric pressure respectively. Nonetheless, the AVUS needs to condense the vapors in order to separate and store them. By using a combination of increased pressure and decreased temperature, AVUS is able to condense fuel vapors, separate them from the air, and easily store them. In order to achieve this, AVUS incorporates a compressor and condenser that are capable of condensing the highly volatile vapors and handling an elevated flow rate during periods of high vapor generation rates, such as hot days and refueling.

Air/Fuel Separation and Condensate Storage

Once the air and gasoline vapors from the gasoline tank have passed through the compressor, the pressurized mixture is sent to the air/fuel separator. The air/fuel separation subsystem is composed of only a condenser, separator, and a storage tank. The mixture first flows through the condenser/heat exchanger to remove additional heat and facilitate condensation. The now cooled and pressurized mixture is flashed into a separator capable of pressures over 790 kPa (115 psia).

Gravity and the difference in density between the remaining vapors and the condensate separate the liquid fuel from the non-condensables. When the pressure within the separator reaches a maximum limit the system releases remaining air/fuel vapors to a modified carbon canister. Unlike the conventional carbon canisters used today, an AVUS canister needs to be able to handle a large percentage of the most volatile hydrocarbons; however, the total surface area of the canister will need to be decreased due to the limited

volume of hydrocarbons that will be needed to be captured. As air and non-condensable vapors are removed from the separator, the liquid hydrocarbons are continued to be collected in the separator until they reach a minimum fill level then sent to a storage tank for later use. To insure that no air or vapors are transferred to the storage tank, the fill level within the separator is continuously monitored.

Fuel Delivery

In order for the AVUS to be a viable alternative to traditional cold starts, the system must insure that the vehicle actually starts on the AVUS condensate and that the starting fuel is not contaminated. Otherwise cold start emission reduction may not be realized to its potential. In order to achieve this, an AVUS vehicle will incorporate parallel fuel injection systems that will supply the cylinders with high pressure fuel. A traditional fuel system uses a fuel pump to supply fuel to the fuel rail, and regulator to control the pressure; however, because the AVUS fuel is vastly different and contamination must be avoided, a common fuel delivery system cannot be used. Ideally, AVUS fuel would use a separate fuel rail, pump, regulator, and injector. From a cost standpoint, the ideal of a dedicated fuel system is an overwhelming task; therefore, the practical application will be left to auto manufacturers while concept and theory will be presented here.

Safety Considerations

The very nature of AVUS operation has the potential to produce an air/fuel mixture capable of being readily ignited. It is not uncommon for air/fuel mixtures to be stored on the vehicles; however, the mixtures are not stored at elevated temperatures and pressure as they are in AVUS. Storing a pressurized mixture of air and fuel, possibly at

elevated temperatures, the separator presents the greatest risk of ignition. Although the majority of the fuel is present in the liquid form, a pre-mixed air/fuel mixture exists that may fall within the flammability limits. The upper and lower limits for 100 octane gasoline are 1.4 and 7.6 percent volume in air respectively. These limits are a function of mixture composition, temperature, and pressure; the limits widen with increased temperature and pressure as seen in the AVUS separator.

In order to significantly reduce ignition risk, AVUS uses a small volume separator. Pressure builds faster in the smaller volume and AVUS would quickly remove any air present in the system. Furthermore, there is only a limited amount of air available in the fuel tank. After several iterations, AVUS would have removed most of the air from the fuel tank and raise the air/fuel ratio above the flammability limits. Another method to raise to raise the mixture above the limit is to maintain a rich mixture within the separator. All of these methods could prevent ignition. In the case that ignition does occur, a smaller volume decreases the available fuel for combustion. Pressure and temperature could also be controlled to reduce risk of ignition but that is work for a later study.

Chapter 3 CONCEPT VALIDATION

Introduction

As the practical concept of AVUS has previously been validated by the work of Alff and Ashford, this chapter focuses on the basic theoretical concept behind AVUS: gasoline vapors and their composition. This chapter seeks to explore the very composition of commercial gasoline and its vapor under normal conditions. Discussion of previous work that supports the theory behind AVUS will be presented, as well as reasons and justification for the simplification of the AVUS test fuel from commercial gasoline to a major component fuel.

Gasoline and Gasoline Vapor Composition

Vapor composition is a function of the parent fuel composition. Using Southwest Research Institute's ASTM D6729 test, Alff found that winter blend Chevron 87 octane gasoline and its AVUS condensate had the compositions found in Figure 4. The parent fuel in this 110 minute test reached a maximum temperature of 52 °C.

Alff and Ashford encountered several setbacks in the compositional analysis of their parent, condensate, and residual fuels. Due to the complexity of the fuels, ASTM D6729 testing was costly and only a limited number of samples could be analyzed. Furthermore, in addition to the percentages shown in Figure 4, 21% of the tested condensate sample was unidentified. However, the results showed the expected trends: an increase in light hydrocarbons from the parent fuel to the condensate from 36% to 58%,

and a decrease in light hydrocarbons in the residual fuel. A significantly higher concentration of light hydrocarbons such as C4, C5, and C6 are present in the condensate than in the parent gasoline; however, heavier compounds were still present. This composition presents the opportunity to reduce cold start emissions by decreasing over fueling that occurs in the initial engine cycles. However, because 21% of the condensate sample is unidentified the results are truly inconclusive.

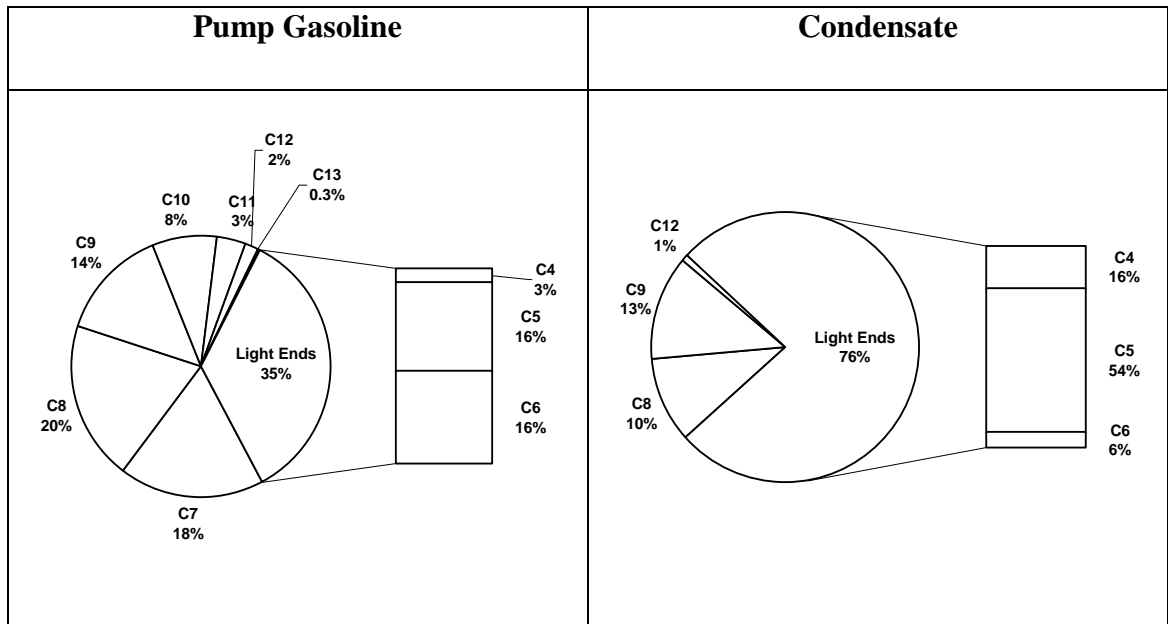


Figure 4. Carbon number breakdown of pump gasoline and AVUS condensate (Alff, 2007)

In a study conducted more recently in Seoul, South Korean, Na *et al* (2004) blended five major gasoline brands by market share in that area. This was done for summer, winter, and spring gasoline. A sample blended mixture was then placed in a 250 mL flask and immersed in a constant temperature bath for 20 minutes. After equilibrium was reached, a sample of the vapor space above the gasoline was removed and analyzed. To validate the tested composition, the vapor composition was also computed using Raoult's Law which allows compositional analysis to be done based on the vapor

pressure above the gasoline mixture of known composition. The law assumes that that the vapor pressure is dependent on the vapor pressure of each chemical component and the mole fraction of the component present in the solution. A mixture that follows this assumption is said to be ideal. The analysis based on Raoult's Law was compared to the experimental data and it was found that the vapor composition can be accurately calculated based on a known liquid gasoline mixture. Composition results based on carbon number for the winter, spring, and summer gasoline blends were very similar, so the averaged results are presented on the following charts. The winter, spring, and summer tests were conducted at 0 °C, 11 °C, and 24 °C respectively (Na *et al*, 2004).

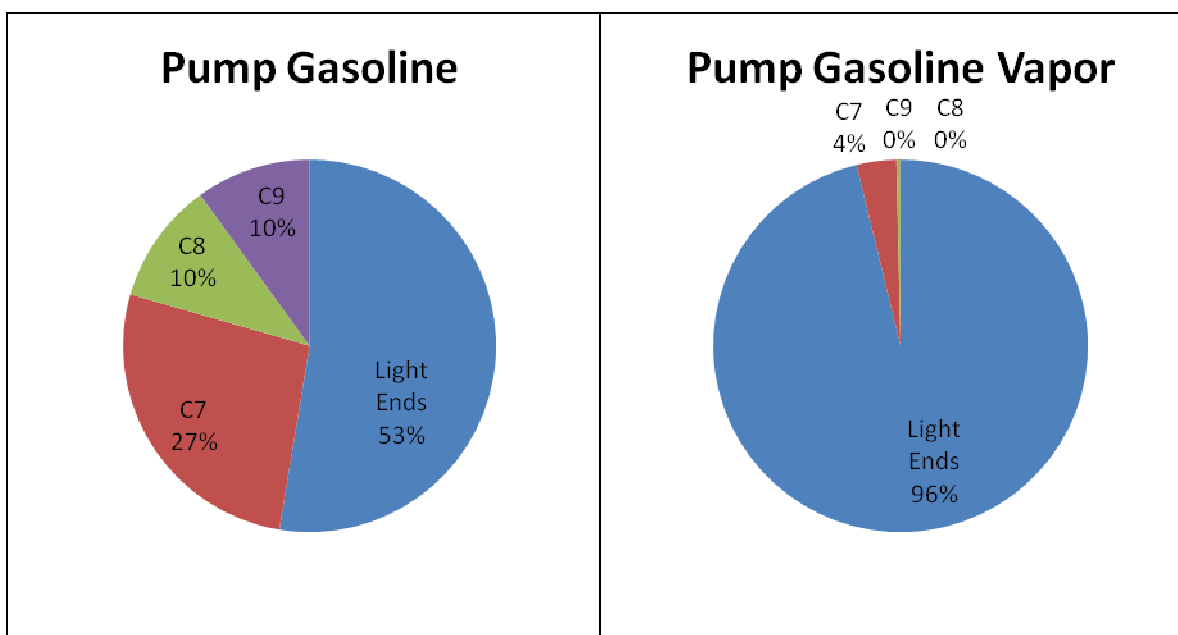


Figure 5. Comparison of compositions of pump gasoline and gasoline vapors (Na *et al*, 2004)

Further detailed analysis showed that for the pump gasoline, the light ends are mostly composed of C5 (24%) and C6 (22%), while the vapor is composed mostly of C4 (39%) and C5 (43%). There is also a significant increase in the percentage of alkanes and alkenes in the vapor while the percentage of aromatics is reduced. Alkanes increase from

56% to 78%, and alkenes from 8% to 18%, but aromatics decreased from 32 to 1.5%. Even at these low temperatures, gasoline vapors present a valuable source of light hydrocarbons that can be used for cold starts (Na *et al*, 2004).

It should be noted that the Seoul gasoline blends had a higher percentage of light hydrocarbons than seen in Alff's study, yet this difference does not discredit the potential of a vapor recovery system such as AVUS. Na's vapors have higher concentrations of light hydrocarbons not only because of the increased light end hydrocarbons in the parent fuel, but more importantly because the tests were conducted at lower temperatures. Lower temperatures mean that the boiling points of many of the heavier hydrocarbons were not reached and therefore those components did not vaporize to a great extent. In practice, AVUS would not have control over the temperature of the gasoline within the fuel tank and therefore heavier components of the gasoline will vaporize; however, the lighter components should vaporize at a faster rate and represent a majority percentage of the starting fuel.

Major Component Fuel

Even if 100% of the AVUS sample tested by Alff and Ashford had been identified, batch production of this AVUS condensate produced from commercial gasoline would have been difficult due to the complexity of the fuel. To alleviate the problems with the compositional analysis encountered by Alff and Ashford, a simplified five component fuel was used as the parent fuel. For E85 tests, the tested fuel was 15% major component fuel and 85% anhydrous ethanol. Furthermore, because the analyzed condensate is composed of only a limited number of species, it will be unproblematic to recreate the fuel in large batches for actual cold start tests. A simpler fuel was much less

expensive to analyze and the limited number of species makes the analysis less complicated.

In order to carefully design a multi-component fuel to model California phase II gasoline, researchers at the Massachusetts Institute of Technology (MIT) divided the hundreds of gasoline components into several groups based on carbon number and type of organic compound (alkanes, alkenes, aromatics). Once separated, the components in each group were represented by the most abundant species of the group. The single species takes on the weight percentage of the whole group. The distillation curve resulting from 15 component fuel matched well with the actual distillation curve of California gasoline (Santoso, 2002).

In a study to model the evaporation process of multi-component fuels at Doshisha University, Senda *et al* (2000) found that hydrocarbons with lower boiling points evaporate at higher temperatures than their own boiling point while those with higher boiling points evaporate at lower boiling points. It appears that the evaporation of lighter hydrocarbons is inhibited by the heavier hydrocarbons. At temperatures below 60 °C the small percentage of light hydrocarbons is held in mixture by the heavier hydrocarbons and no vapor condensate was able to form (Senda, 2000). This major component fuel was created for the purposes of modeling a measuring the evaporation process of multi-component fuel and was not meant to imitate the composition of commercial gasoline.

By regrouping the 15 components of the MIT fuel by carbon number only, the AVUS major component fuel was formulated to contain 25% iso-pentane, 17.5% hexane, 17.5% heptanes, 22.5% iso-octane, and 17.5% toluene by volume. This MDA mixture,

named so after being approved by Dr. Marcus Ashford, was tested with the AVUS and condensate production rates were comparable to those seen for commercial gasoline.

A comparison of the composition of several fuels is presented in Table 1. The components are separated as aromatics and by carbon number. Santoso's MIT fuel contained 13% methyl tertiary butyl ether (MTBE), a gasoline additive used to increase octane rating; yet because of the environmental and health concerns its use has been discontinued in many states. It has been found to easily dissolve in water and contaminate large quantities of groundwater when MTBE gasoline is spilled or leaked at gas stations or leaked from underground storage tanks. Therefore, MIT's 13% MTBE is counted under C5 for fuel comparisons.

Table 1. Comparisons of Major Component Fuels by Carbon Number (Santoso, 2002; Senda, 2000; & Na, 2004)

Component	Santoso- MIT (% mol)	Senda- Doshisha U (% mol)	MDA Fuel- U of AL (% mol)	Na- Yonsei U* (% wt)
C3				0.1
C4	2.0	4.0		3.7
C5	29.6	35.0	28.2	18.1
C6	10.6	12.0	17.3	19.7
C7	11.9	6.0	15.5	14.8
C8	16.1	12.0	17.6	3.7
C9	2.6			0.3
C10	0.7			
C11	0.4			
C12	0.3			
Aromatics	25.8	30.0	21.4	37.2

*All values are presented in percent moles except results from Yonsei University which are in percent weight.

The MDA fuel is comparable to the MIT California model fuel; the MDA fuel contains 45.5% lights while MIT fuel contains about 43% light ends. The mix of light hydrocarbons is also similar; however, the MIT fuel contains a very small percentage of

heavier hydrocarbons that the MDA fuel does not contain. The MDA five component fuel should simplify analysis while reasonably mimicking commercial gasoline.

The chemicals used to produce the MDA five component fuel and its E85 derivative are HPLC grade iso-pentane, hexanes, n-heptane, 2,2,4 trimethylpentane, toluene, and anhydrous ethanol. All chemicals were purchased from Fisher Scientific. Species were measured and mixed using 500 mL graduated cylinders.

Chapter 4 EXPERIMENTAL SETUP

Introduction

This chapter details the experimental apparatus and method of testing that was used to create AVUS cold start condensate from the vapors of the MDA five component fuel. Unlike previous work done with the AVUS, this study only reflects a single AVUS configuration. The AVUS configuration used here has slight modifications to the version used by Alff and Ashford, but will be referred to only as AVUS. For detailed information on previous AVUS configurations see “Experimental Study of an Active Vapor Utilization System for Use in Gasoline Powered Vehicles” by Michael Alff.

AVUS Experimental Apparatus

The goal of the AVUS setup is to use small reliable components that could be placed on a vehicle if desired. As mentioned previously, the major components of AVUS are a fuel tank, compressor, condenser, air/fuel separator, and condensate storage tank as seen in Figure 6. In order to mimic temperature profiles seen on vehicle, the bench top AVUS apparatus also uses adjustable hotplates to warm the fuel at an acceptable rate.

The experimental AVUS fuel tank is a 15 L (4 gal) aluminum fuel tank. This tank provides multiple inlets and outlets that were used for vapor retrieval and recirculation, liquid fuel recirculation, fuel temperature measurement, pressure measurements, and nitrogen purges. The tank is capable of withstanding small pressure increases that may occur from the increase in vapor from the warmed fuel. Two temperature controlled hot

plates are placed under the tank and are used to heat the fuel during vapor production. In order to prevent uneven heating and hot spots, a 19 mm (3/4 ") thick aluminum plate is placed between the hot plates and the fuel to tank to act as a heat distributor. Ideally, the aluminum plate would more equally disperse the heat from the hot plates to the lower surface of the fuel tank. All AVUS tests are conducted under a fume hood which causes accelerated air flow. To prevent the cold spots caused by the heat loss from the sides of the fuel tank, insulating tape was used to cover all surfaces of the fuel tank exposed to the circulating air.

As the fuel begins to warm, vapors are allowed to form inside the fuel tank until a predetermined pressure upper limit is reached, then the compressor is activated and vapors are removed until the lower fuel tank pressure is reached. This process repeats for the duration of the tests. In order to handle the rate of vapor production from the four gallon fuel tank, a sample dual head diaphragm compressor is used for vapor removal. To achieve the target output pressures of about 790 kPa (115 psia), the dual heads of the compressor are configured in series; however, this series configuration has a decreased flow capacity when compared to the parallel configuration. The compressor is only capable of starting when the downstream pressure is below 240 kPa (35 psia), which caused problems when the separator pressure exceeded this threshold and the fuel tank vapors needed to be removed. To solve this problem a three-way solenoid and a check valve are placed in line between the compressor and the condenser. The check valve prevents vapors from blowing back into the compressor. After each operation of the compressor, the three-way valve is momentarily opened to relieve the additional unwanted pressure downstream of the compressor. The removed pressure and vapors are

re-circulated back to the fuel tank which is at a much lower pressure. Even though the removed vapors may be at a much higher pressure than the fuel tank, the small volume of the vapor prevents the fuel tank from seeing a significant change in pressure. The chosen dual head diaphragm sampling compressor uses a 12 V DC power source and is capable of producing pressure up to 790 kPa and flow rates up to 36.5 L/min.

Once the pressurized vapors leave the compressor they enter a thermoelectric condenser. The AVUS condenser is a 200 W solid state condenser that uses Peltier coolers. The air/liquid electric cooler is capable of removing heat from a fluid medium whether it is transient or stationary within its tubing. The condenser runs continually, regardless of the compressor activation; however, flow through the condenser is controlled by the compressor. The previous AVUS was configured so that the tubing connecting the bottom of the condenser to the bottom of the separator was horizontal so that the collected liquid and vapor could be continuously cooled, yet was found that liquid backed up in the condenser and distorted the condensate collection rate and possibly caused compression problems within the separator. To fix these problems, the current AVUS is configured so that the condenser's outlet tubing connects to the top of the separator which has been lowered beneath the condenser. This allows for all liquid to collect in the bottom of separator without interference from incoming vapors.

The AVUS separator is a stainless steel double-ended DOT-compliant sample cylinder capable of withstanding pressures up to 12,410 kPa (1800 psig). Once the vapor/liquid mixture enters the separator, hydrocarbon vapors begin to condense and air, along with other non-condensed vapors, rise to the top of the tank. The condensed liquid level is manually monitored using a clear sight glass located adjacent to the separator. As

mentioned previously, the vapor inlet of the separator is located at the top of the cylinder; also connected there are a pressure transducer and a solenoid pressure release valve. For the experimental setup, the excess pressure is vented to the atmosphere under the fumed hood, but in practice these non-condensed vapors would be released into a specialized carbon canister. The separator pressure release operates similarly to the fuel tank. Pressure is allowed to build within the cylinder under an upper limit is reached, and then a solenoid valve is momentarily opened to allow a portion of the uncondensed vapors to escape. This setup is depicted in Figure 6.

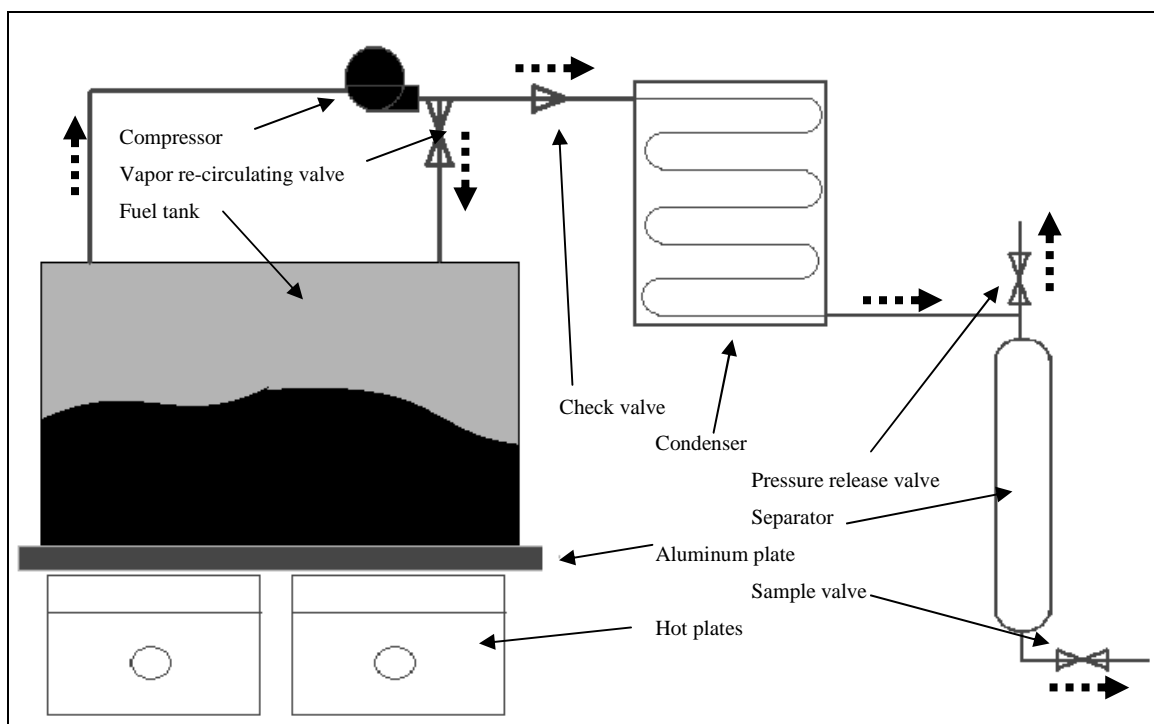


Figure 6. Experimental setup of the AVUS

Unlike the previous AVUS setup, the liquid fuel in the separator is not sampled when a predetermined volume is collected. The condensate from that AVUS was not sampled until enough condensate had been produced for a 4 mL sample. Usually this would occur 70 minutes into the 80 minute test. Due to adjustments in the operation of AVUS and the amount of tested fuel, the condensate is being produced at a much faster

rate; however, samples are not taken until the end of the 90 minute test, regardless of the amount of sample produced. In fact, information about the volume of sample produced during each test is used to characterize results and will be presented in the chapter on results and discussion.

AVUS Preparation

Before each AVUS experiment a leak check is performed on the system. A dedicated LabView routine is used to test the correct operation of the solenoid valves and compressor as well as pressure test the system for leaks. Each section of the system is pressurized with nitrogen and closed off from the remainder of the system and watched for continuous pressure drops which would indicate a leak.

For the fuel tank, nitrogen is introduced from a gas cylinder. Once the upper pressure limit of 138 kPa (20 psia) is reached the nitrogen supply is disconnected and the tank pressure is watched for any drops. If the pressure remains stable, the fuel tank passes the pressure check and the separator is then tested. The pressure is removed from the fuel tank using the compressor and stored in the sealed separator. The air/fuel separator solenoid used to relieve pressure downstream of the compressor is also checked for correct operation during this process. Additional nitrogen is added to the system until a pressure of 790 kPa (115 psia) is reached in the separator. Once the testing pressure is reached the system is closed and watched for pressure drops. After the separator passes the pressure test, the excess nitrogen is released from the system by the solenoid at the top of the separator. All pressures within the system are returned to atmospheric.

AVUS Operation

After the preparation procedure is completed, 2 L of MDA five component fuel is added to the empty fuel tank. To avoid excess evaporation of fuel components, the MDA fuel is mixed directly into the fuel tank. The capacity of the fuel tank is 15.14 L, so with 2 L of fuel there is a vapor space of 13.14 L. This large vapor volume along with the small volume of fuel that must be heated by the hot plates, explains the increased vapor recovery rate of the current AVUS over the previous AVUS. The tank is sealed and pressurized with nitrogen during setup. Once the pressure in the tank reaches the upper limit the compressor is activated. The pressure from the tank is transferred to the separator by the compressor. Once the separator reaches its upper limit the nitrogen/air mixture is purged from the system. This process continues for several cycles before the nitrogen is disconnected. The compressor continues to run until the pressure within the tank reaches the lower limit. This secondary preparation procedure also removes a majority of the air from the system before testing helping to reduce ignition risk before the fuel temperature and pressure are elevated.

For the 90 minute test on MDA fuel, the hotplates were manually set at a heat setting of 100 for the first 45 minutes and 125 for the remainder of the test. The setting on the hotplates do not directly correlate to a temperature so several initial tests had to be performed to find a suitable heating profile that resulted in final temperatures near 60 °C. This same heating procedure was maintained for all tests performed on the MDA fuel regardless of the actual fuel temperature. The goal of this artificial fuel heating is to mimic fuel temperature that would be typically seen on a vehicle. Figure 7 shows a temperature profile observed during Sealed Housing for Evaporative Determination

(SHED) testing. The tested drive cycle consisted of one LA-4 driving schedule, followed by two minutes idle, two NY cycles, two minutes idle, and one LA-4 driving schedule. Over the course of the test, the temperature of the fuel increases from an ambient temperature of about 32 °C to a final temperature near 60 °C. AVUS experimental temperature profiles will follow similar trends.

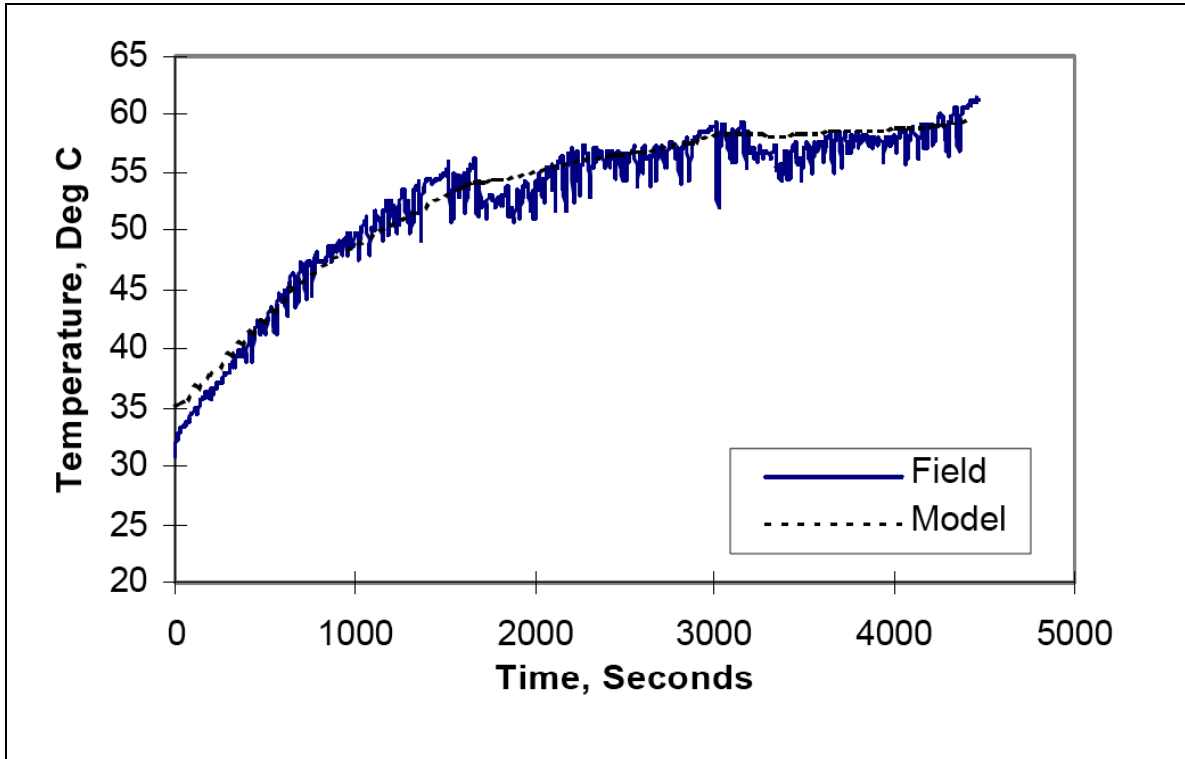


Figure 7. Fuel temperature profile as seen by during SHED testing (El-Sharkawy, 1998).

The upper pressure limit within the fuel tank is maintained at 107.9 kPa (15.7 psia) throughout the duration of the test. As the fuel reached higher temperatures the evaporation rate increased as expected which resulted in less time between compressor activation and in some cases, prolonged compressor operation. Special care was taken to prevent compressor overheating in these cases. The lower fuel tank pressure is set at 101.3 kPa, atmospheric. In practical application, the upper pressure limit of the fuel tank could be adjusted to prevent compressor overheating while collecting vapors at a suitable

rate. The pressure within the air/fuel separator operates on a similar principle as the fuel tank except the upper and lower pressure limits are much higher. In preliminary AVUS tests the separator pressure limits were set between 618 and 549 kPa (80 and 90 psia). The limits were later increased to 720 and 790 kPa (105 and 115 psia) in order encourage condensation within the separator. Temperature and pressure data were collected for each run and will be discussed in a later chapter.

E85 AVUS Operation

For E85 tests the fuel tank is filled with 1.70 L of anhydrous ethanol and 0.3 L of premixed MDA five component fuel. Because of the decreased heating rate of the E85 fuel, a different heating profile was chosen for tests on this fuel. For the 90 minute test, the hotplates were manually set at a heat setting of 100 for the first 45 minutes, 125 for the next 25 minutes and 150 for the remainder of the test. All other operating parameters are identical to 100% MDA fuel operation.

Chapter 5 TESTING, RESULTS AND DISCUSSION

Introduction

The very operation of AVUS aims to produce a highly volatile fuel that can be used in cold starts to reduce hydrocarbon emissions, yet the evaporation of these light species ultimately changes the composition of the parent fuel. AVUS operation should not significantly alter the makeup of the parent fuel as only a small percentage of fuel is removed. Furthermore, the species that are removed are those which would have normally been lost to the atmosphere or collected in the carbon canister. The effect of AVUS on the parent fuel and the composition of the AVUS condensate must be quantified. A detailed hydrocarbon analysis based on carbon number was performed on the condensate and the residual fuel to analyze samples taken from AVUS. In order to find an alternative but effective way to measure composition and ethanol content, refractive index and infrared adsorption measurements were also taken.

This chapter discusses the tests performed with the AVUS, the MDA five component fuel, ethanol mixtures, and the AVUS condensate samples. The data collected from the actual AVUS experiments includes pressure and temperature profiles. The AVUS condensate and residual fuels were tested for index of refraction, infrared absorption and hydrocarbon compositional analysis. Data has been collected on a total of 12 AVUS experiments. Fresh 2 L batches of both MDA fuel and MDAE85 fuel were run three times each. Each set of fuel was then run two successive times to observe the effect

of running AVUS on gasoline that has already had portions of the light ends removed through vapor extraction. Therefore, each original batch of fuel has had three experiments run on it. AVUS samples produced from MDA fuel are series A and B, while the samples produced from the E85MDA fuel are labeled C and D. The first, second, and third sequential test on the A series of tests are labeled A-01, A-02, and A-03 respectively. The residual fuel from the A series is labeled A-R. The same labeling system is used the B, C, and D series. After each test, the fuel tank and separator were allowed to return to room temperature. At the completion of the third test the residual fuel in the fuel tank was removed and measured for volume. The final section of the chapter will offer a discussion of the results and trends observed across the various tests.

Temperature and Pressure Profiles

Temperature

As mentioned previously, the heating of liquid gasoline is controlled by the use of two hotplates. Every attempt was made to maintain standard temperature profiles from one AVUS experiment to the next, but unfortunately uniform temperature curves for each test could not be achieved. Figures 8 and 9 show the averaged temperature profiles for successive runs on either fuel. MDA-1 denotes the averaged first run of MDA fuel tests; MDA-2 denotes the averaged second run on the same fuel, et cetera. The MDAE85 experiments follow the same pattern. For each test, the liquid fuel starts at temperatures near 25 °C depending on the ambient temperature of the laboratory. Over the course of the 90 minute test, the fuel temperatures steadily increase to final temperatures near 65 °C. Slight discontinuities can be seen in the temperature curves as the heating rate on the hot plates is increased. It should be noted that as successive tests are performed on the

same batch of fuel, the amount of fuel remaining in the fuel tank is decreased and therefore warms faster. Though this change in volume is minimal, it may explain a portion of the uniformity of the temperature profiles.

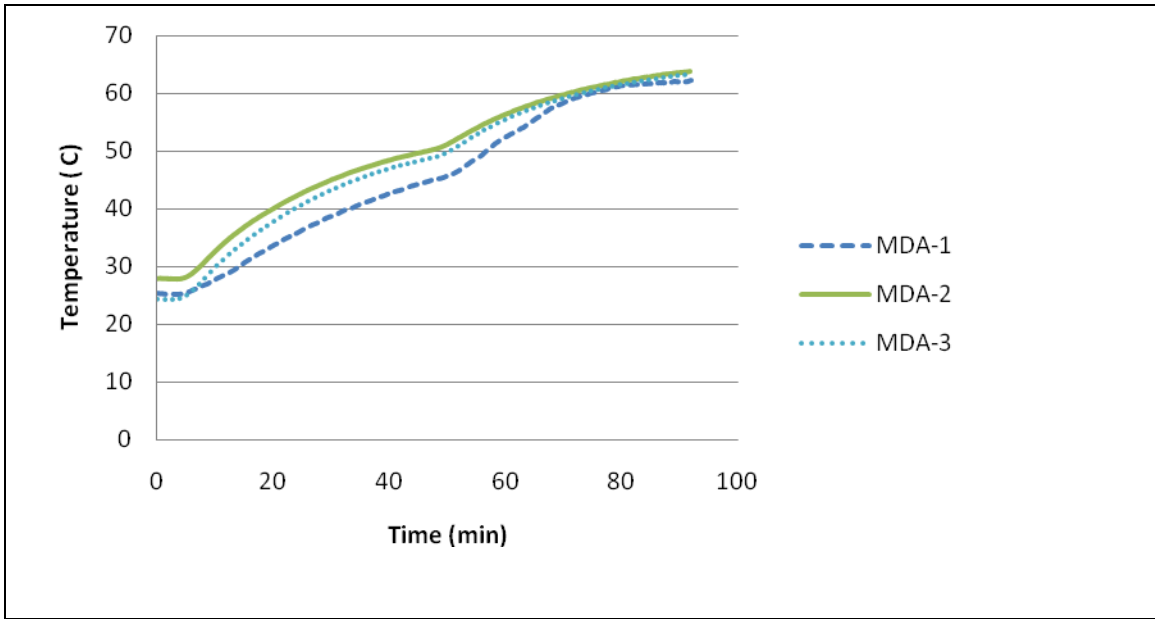


Figure 8. Fuel temperature profiles from AVUS experiments on MDA fuel

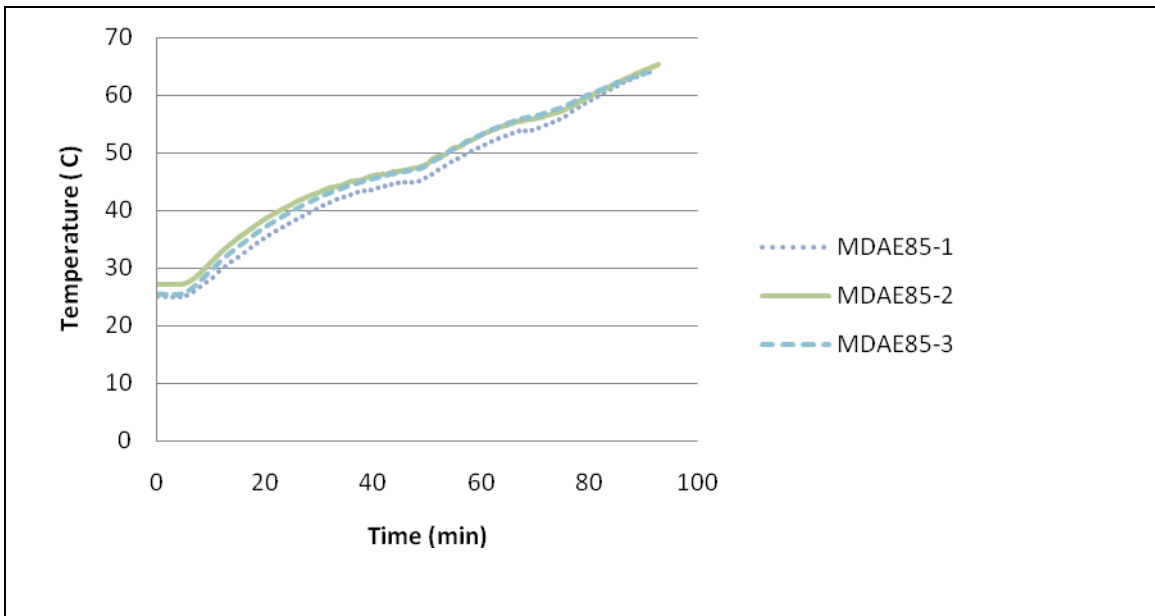


Figure 9. Fuel temperature profiles from AVUS experiments on MDAE85 fuel

In any given set of AVUS tests, the greatest difference in temperatures is near 5 °C. Though this is a small difference, it has significant effects on the AVUS condensate collected. Iso-pentane, the major component that should be present in the AVUS condensate, has a low boiling point of 28 °C, AVUS experiments with higher temperature profiles should expect to see lower concentration of iso-pentane because the heavier MDA fuel components begin to vaporize. However, the higher temperatures increase the total vaporization rate and lead to greater volumes of AVUS condensate collected.

Pressure

Figure 10 shows pressure profiles taken from an AVUS experiment performed on a fresh batch of MDA fuel. This pressure profile is representative of pressure profiles seen throughout the series of experiments.

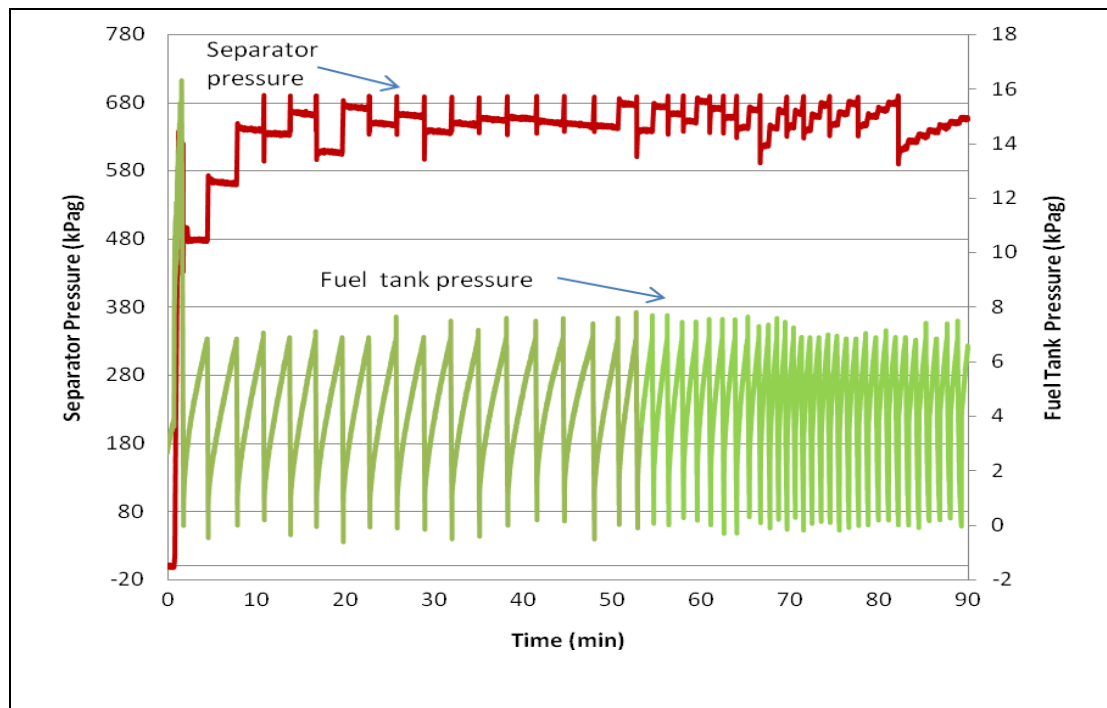


Figure 10. Fuel tank and separator pressure profiles

The negative values at the start of the test are inaccurate values read by the data collection system before the pressure transducers were turned on. Notice that the readings for both the fuel tank and separator immediately increase at the start of the test then decrease as vapors are removed from either component of the system. The only difference between the pressure readings taken in Figure 10 and other tests is whether or not the nitrogen purge, which manifests as increased pressure readings in both the fuel tank and the separator, is recorded during the collected data. This purge has no effect on the collected data as it occurs before all AVUS tests.

As the experiment begins, the pressure in the fuel tank builds as a result of heating until the pressure reaches 107 kPa (1psig) at which point the compressor activates, removes a portion of the vapors from the fuel tank, and increases the pressure within the separator. This process repeats for the duration of the 90 minute test. However, the expected and interesting occurrence is the elapsed time between these cycles. As the fuel heats, the time it takes to reach the upper limit within the fuel tank decreases indicating an increase in vaporization rates.

Once the separator initially reaches its upper limit of 789.5 kPa (100 psig), the separator experiences its pressure releases in conjunction with the activation of the compressor. However, towards the end of the test, multiple runs of the compressor are needed to reach the upper limit of the separator after pressure release. This is indicative of the vapors leaving the fuel tank having a higher concentration of condensable species. As the compressor runs it is actually compressing the vapors back to liquid form instead of simply just moving gaseous species from the fuel tank to the separator. During the

experiments, this phenomenon coincides with a rapid condensate production in the separator.

Table 2. Average temperatures and pressures

Sample Number	Time Averaged Fuel Temperature (°C)	Time Averaged Fuel Tank Pressure (kPag)	Time Average Separator Pressure (kPag)
A-01	46.51	4.32	501.94
A-02	50.40	4.06	405.07
A-03	48.15	4.05	414.31
B-01	45.59	4.59	635.83
B-02	50.70	3.75	433.20
B-03	49.06	4.01	435.40
C-01	49.05	4.14	653.83
C-02	48.15	4.14	612.74
C-03	47.32	3.87	629.08
D-01	46.61	4.07	581.57
D-02	47.06	3.94	640.52
D-03	47.41	3.59	625.56

Refraction Results Testing and Results

Relative refractive index is the ratio of the speed of light in one medium to the speed of light in an adjacent medium. Many substances such as gemstones, liquids, transparent solids, and hydrocarbons have characteristic refractive indexes and can be identified by these values. For this study, the constant medium is air and the adjacent medium is the liquid hydrocarbon samples. Several studies have found that refractive index and emitted wavelength may be suitable measures of content of hydrocarbon mixtures (Brocos, 2003; Chen, 2005; Falate, 2003). In fact, Falate *et al* states that a fiber optic long period grating sensor beneficial application in the Oil and Gas Industry because of their non-electrical long range possibilities (Falate, 2003). All of these studies state that the refractive index of the mixture is dependent on the volumetric

concentrations of its constituents. Deviation from the volumetric average of refractive indexes is given by:

$$\Delta n_D = n_D - \sum_{i=1}^N \phi_i n_{Di} \quad (1)$$

with

$$\phi_i = \frac{x_i V}{\sum_{i=1}^N x_i V_i} \quad (2)$$

For these equations, n_D , n_{Di} , and ϕ_i are the refractive index of the mixture, the refractive index of the species i , and volumetric fraction of species i , respectively. N is the total number of pure species within the mixture, V is the total volume, V_i is the volume of species i , and x_i is the mole fraction of species i (Brocos, 2003). Previous studies have used this technique for binary and ternary mixtures so additional analysis will be needed to relate the concentrations of each of the five or six components to the measured index of refraction of each sample.

The refractive index of most AVUS samples was measured three times and averaged. The averaged index was then compared to the averaged volumetric refractive index based on the GC hydrocarbon analysis. Samples less than 10 mL were not tested with refractive index because the entire sample had to be sent off for GC analysis.

Past studies have shown that for binary mixtures, the measured index of refraction varied from the volumetric average of the index of refraction but in a predictable pattern. The volumetric average of the index of refraction is the sum of the products of the volumetric averages and refractive indexes for each respective species. Therefore, given

the measured index of refraction and the two constituent hydrocarbons, a composition could be determined as there is only one unknown variable. It was hypothesized that the MDA five component fuel could be treated as a single component in a binary mixture with ethanol and the ethanol content could be predicted with reasonable accuracy. As the composition of the MDA fuel is constant, it too has a characteristic index of refraction. The index of refraction for each component of the MDA fuel, as well as the MDA fuel, was measured. Each of the hydrocarbon species used was found to have measured values that correspond well with accepted values. A comparison of measured and accepted values can be seen in Table 3.

Table 3. Measured and accepted index of refraction values

Species	Experimental	Published	Difference (%)	Standard Dev
2-Methylbutane	1.35473	1.35370	0.00076	0.000289
Hexanes*	1.38000	N/A	N/A	0.000100
Heptane	1.38677	1.38550	0.00091	0.000208
Toluene	1.49430	1.49410	0.00013	0.000361
2,2,4-Trimethylpentane	1.39077	1.38840	0.00170	0.000379
Ethanol	1.36277	1.36110	0.00122	0.000208
MDA fuel	1.40070	N/A	N/A	0.000252

*Hexanes used in this study is a mixture of hexane isotopes therefore accepted index of refraction could not be determined for the mixture.

AVUS condensate samples are also measured for refractive index and deviations from the volumetric average are calculated. However, as the AVUS condensate is not a simple mixture of two species, but a blend of six hydrocarbons in various ratios. Index of refraction alone cannot be used to determine composition, but composition can reasonably determine index of refraction.

Ethanol Blends

Ethanol and MDA 5 component fuel are mixed in 100 mL combinations from 0 to 85% ethanol by volume in 15% increments. The remaining volume is MDA fuel. As the MDA fuel is to be treated as a single component, samples of MDA fuel were measured for refractive index and a characteristic index of refraction of 1.4007 was determined. Three room temperature samples of each MDA-ethanol blend were measured for refractive index and are plotted on Figure 11. As expected, the measured and calculated values for refractive index have very little difference as the concentration of either component nears 100%. The difference between the actual and calculated increases as the concentrations of either component increases with a maximum difference at an ethanol concentration of 30%. However, the difference curve is not as smooth or predictable as the true binary systems studied by Falate, Brocos, and Chen. A portion of this may be due to insolubility of ethanol in the MDA fuel in mixtures with less than 20% ethanol. The interaction between the various MDA fuel components and the ethanol may also cause the index of refraction of the mixture to behave in an unexpected manner. Unfortunately, the scope of this work is to determine the feasibility of refractive index to determine ethanol content. Research into the phenomenon causing unexpected behavior is left for later work.

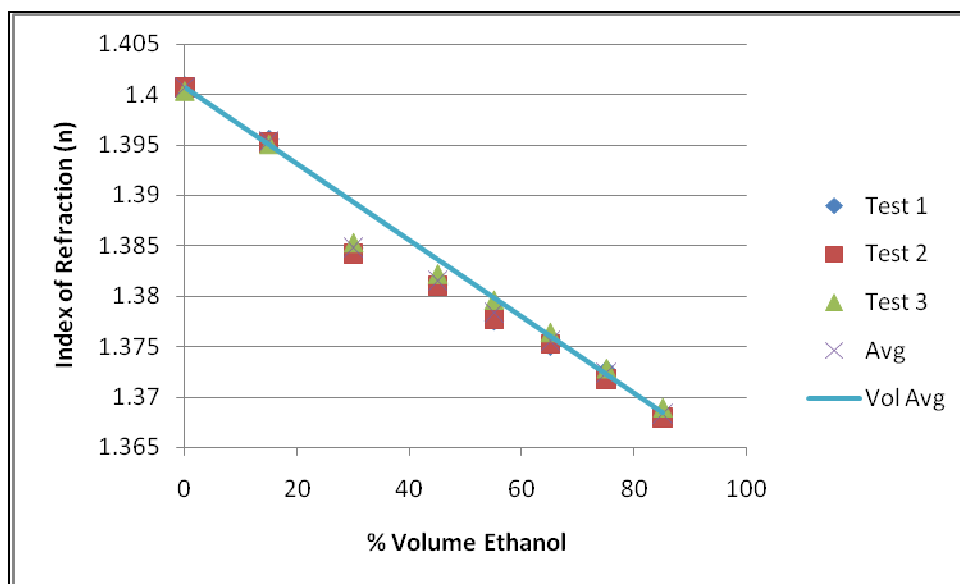


Figure 11. Refractive index and variation of deviation for MDA-ethanol fuels

As the MDA fuel is only a simplified test fuel, 87 octane commercial gasoline from several major refueling stations was collected and measured for index of refraction. Tuscaloosa, AL is in a nonattainment zone, and therefore gasoline may contain up to 10% ethanol by volume. Table 4 shows the results of these tests. All of the collected samples have refractive index higher, but reasonably close, to that of the MDA fuel, 1.407. As ethanol has an index of 1.3611, the index of refraction will decrease and approach 1.36 as ethanol content increases. However, gasoline is a mixture of various hydrocarbons so the deviation from the expected index of refraction will likely be unpredictable.

Table 4. Refractive index for name brand gasoline

Station	Test 1	Test 2	Test 3	Average	Standard Dev
Chervon	1.4178	1.4205	1.4210	1.4198	0.00172
Shell	1.4212	1.4211	1.4212	1.4181	0.00523
BP	1.4179	1.4173	1.4155	1.4169	0.00125
Jet P	1.4141	1.4140	1.4145	1.4142	0.00026
Exxon	1.4134	1.4136	1.4135	1.4135	0.00010

AVUS Condensate

As the AVUS condensate does not have a predetermined and consistent ratio of MDA fuel species, index of refraction is not ideal for determining composition or ethanol content. The hydrocarbon species used to produce the MDA fuel cover an index of refraction range from 1.3537 (iso-pentane) to 1.4947 (toluene). An infinite combination of these fuels could produce a given index of refraction and have varying levels of light and heavy species as well as ethanol content. However, the AVUS is designed to collect the light species of the parent fuel, mainly iso-pentane whose index is the lowest of the MDA species; therefore, higher indices do indicate stronger concentrations of heavier components. The indices of refraction for AVUS samples are seen on Table 5. Samples from the C series are not listed and were not tested as the volume of sample was limited.

Table 5. Index of refraction for AVUS samples

Sample	Test 1	Test 2	Average
A-01	1.3700	1.3695	1.3698
A-02	1.3775	1.3800	1.3788
A-03	1.3794	1.3850	1.3822
A-R	1.4078	1.4075	1.4077
B-01	1.3749	1.3755	1.3752
B-02	1.3739	1.3751	1.3745
B-03	1.3782	1.3806	1.3794
B-R	1.4113	1.4100	1.4107
D-01	1.3726	1.3705	1.3716
D-03	1.3760	1.3765	1.3763
D-R	1.3665	1.3662	1.3664

AVUS condensate samples produced from MDA five component fuel generally exhibit index of refraction values from 1.37-1.38. This trend corresponds with the high iso-pentane concentration found in these samples. However, the residual fuels are

characterized by index of refraction values near 1.41. Of the fuels used to create the MDA fuel, iso-pentane has the lowest index of refraction; in fact, except for toluene, the index of refraction of the MDA hydrocarbons increase with carbon number. Toluene has an index of refraction value near 1.49. The concentration of toluene left in the residual can be linked to the higher index of refraction for those samples. Therefore, lower index of refraction is an indicator of higher the concentration of light hydrocarbons. However, the opposite trend is seen in the samples resulting from the E85MDA fuel. As ethanol has a low index of refraction of 1.36, the AVUS condensate samples actually have higher index values near 1.37. This can be explained by 85% ethanol present in the parent fuel. The strong ethanol concentration lowers the index of the parent fuel while the higher concentration of other hydrocarbons in the condensate increases index. However, as mentioned in a previous section, an infinite combination of the five components of the MDA fuel can result in any index of refraction value so the value alone is not a reliable indicator of fuel composition.

Infrared Testing and Results

The infrared spectra can be used to identify functional groups in organic compounds such as hydrocarbons by using the wave number values of the spectrum. These wavenumbers match a particular frequency of infrared light and specific combinations of frequencies of infrared light are absorbed by certain hydrocarbons. A hydrocarbon molecule absorbs infrared radiation because vibration of the atoms in the molecule produces an electric field that matches the frequency of incident IR light.

The vibrating atoms of the hydrocarbon molecules stretch and bend relative to each other. This movement requires energy and these vibrations occur at specific

frequencies. The relationship between energy and the frequency can be correlated by Planck's constant, 6.6×10^{-34} joule-second, and the equation is $E = h \cdot n$. The parameter h is Planck's constant, n is the frequency, and E is equal to the energy associated with the bond. Each bond within a given molecule has an associated energy, and therefore frequency. Each complete molecule absorbs a unique set of frequencies that match the natural vibration modes of the molecule. This combination is specific to that molecule and can be used to identify a compound.

The infrared spectrum for a molecule shows the frequencies of IR radiation absorbed on the horizontal axis and the percent of the incident light that passes through the molecule without being absorbed. A frequency at which 100% of the light passes through denotes a vibration energy that is not present in the molecule. Areas of the graph where percent transmittance drops to a lower value then rises back to near 100% is called a band and is associated with a particular vibration within the molecule.

All hydrocarbons show a band near 3000 cm^{-1} . The strong bands above 3000 cm^{-1} come from carbon-hydrogen bonds in the CH_2 and CH_3 groups present in most hydrocarbons while the weak band below 3000 cm^{-1} near 1650 cm^{-1} is characteristic of the CC double bond of an alkene. Aromatics can be identified by pi bonds which will have bands characterized by medium to strong absorption bands around $1650\text{-}1450 \text{ cm}^{-1}$. The CH stretch band near 3000 cm^{-1} is much weaker than in alkenes. For alkanes the main absorption will be the C-H stretch near 3000 cm^{-1} . The spectrum will be very simple with another band near 1450 cm^{-1} (Reusch, 1999). Figure 12 shows the difference in infrared spectrum for alcohol and non-alcohol fuels.

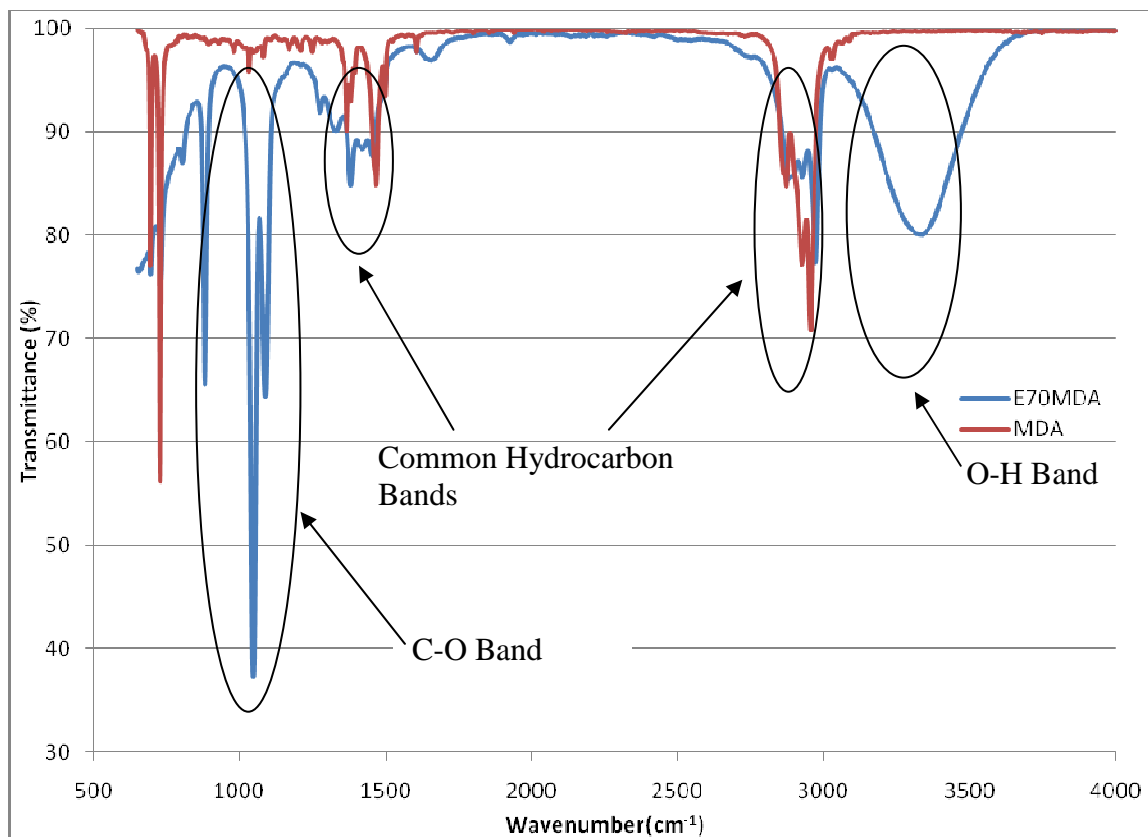


Figure 12. Infrared absorption for alcohol and non-alcohol fuels

Of all the hydrocarbons dealt with in this study, the most identifiable band within the spectrum was that produced by ethanol. Alcohols produce a wide OH band near $3600\text{-}3300\text{ cm}^{-1}$ and a C-O absorption band near $1300\text{-}1000\text{ cm}^{-1}$. Whereas all hydrocarbons have CH bonds, and many have CC double bonds that produce bands in the 3000 cm^{-1} and 1500 cm^{-1} ranges, alcohols produce a distinct band in a range not by exhibited other bonds (Reusch, 1999). This can be readily used to identify alcohol content of a hydrocarbon mixture. For this study, infrared spectroscopy is used a method to indentify the hydrocarbons mixture of the AVUS, and more specifically the ethanol content of samples produced by MDA based E85 fuel.

In order to initially study the practicality of infrared testing to determine alcohol content, various mixtures of ethanol and MDA five component fuel were mixed and tested for infrared spectrum absorption. From these results a correlation between absorption and ethanol content is proposed. The AVUS samples were also tested and the analyzed chemical content is used to determine the validity of the equation predictions.

Phase Separation

Ethanol and MDA five component fuel were mixed in 100 mL combinations from 0 to 95% ethanol by volume. The remaining volume is 100% MDA fuel. While mixing the fuels it was discovered that the fuel did not readily mix and at room temperature certain combinations of the fuels do not completely mix even after shaking. For these combinations two liquid phases are present. To further investigate this phenomenon, the mixtures from 5 to 45% ethanol by volume were allowed to settle at room temperature, in a refrigerator, and a freezer.

When mixing the fuel combinations, the MDA fuel was poured over the ethanol volumes using a pipette so not to disturb the mixture. Before mixing, a distinct layer could be seen in each of the graduated cylinders. After mixing, a layer remained in the mixtures from 10 to 20% ethanol, and these mixtures appeared cloudy until settled. However, the layers were 2, 4, and 5 mL for the 10, 15, and 20 mL ethanol mixtures respectively. This shows that some of the ethanol is absorbed into the MDA fuel, and vice versa. Because of the low volumes of the lower phase for these mixtures and the higher density of ethanol (0.789 g/mL) when compared to the volumetric average density of the MDA fuel (0.697 g/mL), it is assumed that this phase is ethanol rich. The exact composition of each phase cannot be determined without a detailed analysis. Because of

the two phases in the lower ethanol blends, these mixtures cannot be used to correlate ethanol content and infrared absorption.

The ethanol mixtures were allowed to settle at two other temperatures and the volumes of each phase were observed and recorded. In order to be able to observe and measure the phases, the mixtures settled in uncovered graduated cylinders so evaporation of the mixture is a factor to be considered. To combat this occurrence, results are presented in percent of total mixture instead of mL on Figure 13. It should be noted that at the lower temperatures the volume of the denser phase increases beyond that of the ethanol content present for each ethanol blend. It is likely that at those temperatures the solubility of ethanol and MDA fuel components change and species begin to shift from one phase to the other. This experiment was done to qualify the extent of phase separation in the MDA-ethanol mixtures and is not meant to be a detailed analysis. The exact nature of this phenomenon is beyond the scope of this research. The presence of multiple phases complicates the use of IR testing. The dense phase is likely to have a strong ethanol content while the less dense phase will likely fall in the range where IR testing is unproven with the MDA fuel. The composition of these phases will be discussed in a later section.

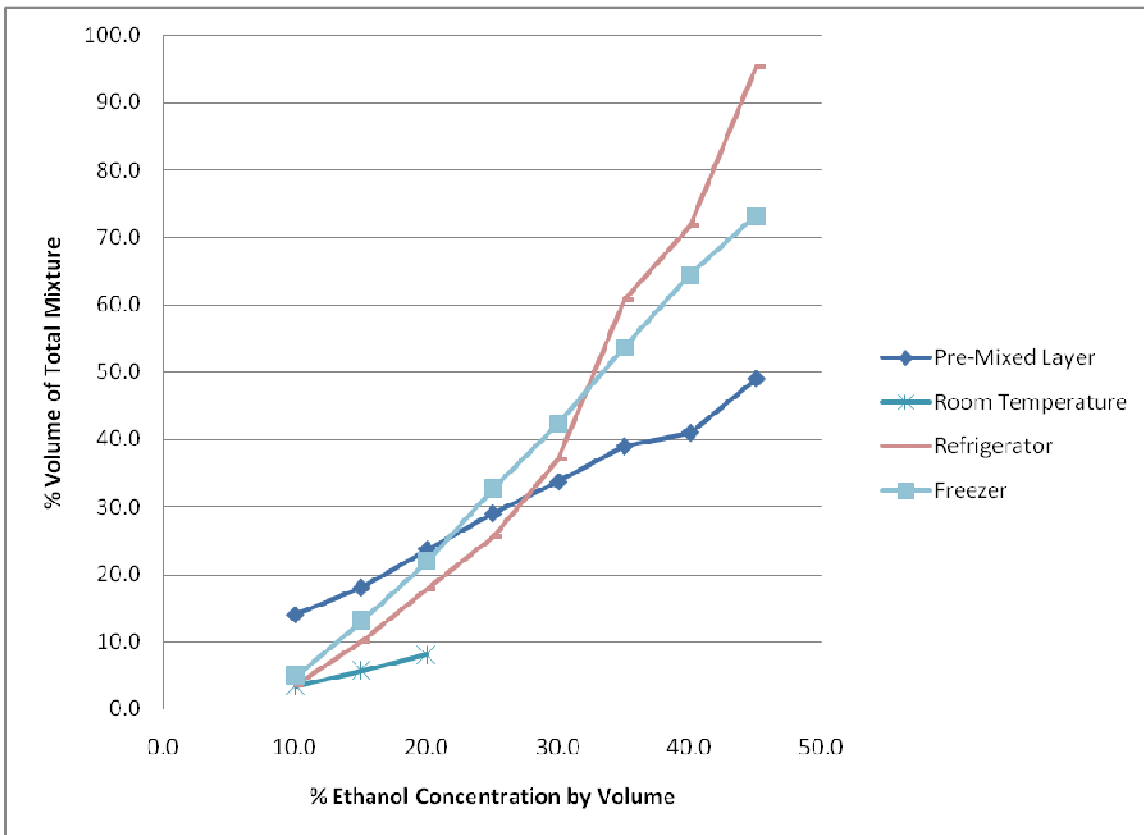


Figure 13. Percent denser phase in ethanol mixtures

Infrared

For ethanol mixtures greater than 30% ethanol by volume, a room temperature sample is used to measure infrared absorption. The strength of the infrared adsorption in the ranges near $3600-3000\text{ cm}^{-1}$ and $1300-1000\text{ cm}^{-1}$ are of particular interest due to the OH and CO bonds found only in alcohols. Other wavelength ranges have absorption due to bonds common to all hydrocarbons and cannot be readily used to determine ethanol content (Reusch, 1999). Furthermore, when analyzing AVUS samples where the concentration of all of the components has changed, it is important to be able to determine alcohol content because of its significantly lower energy content. The results of the ethanol blend tests for the entire spectrum can be seen in Figure 14. Closer looks at

the focus regions can be seen in Figure 15. The results show that for the MDA-ethanol mixtures there is an obvious correlation between ethanol content and the infrared absorption. Percent volume ethanol content is plotted against the minimum transmittance values for each mixture in each of the specified ranges in Figure 16.

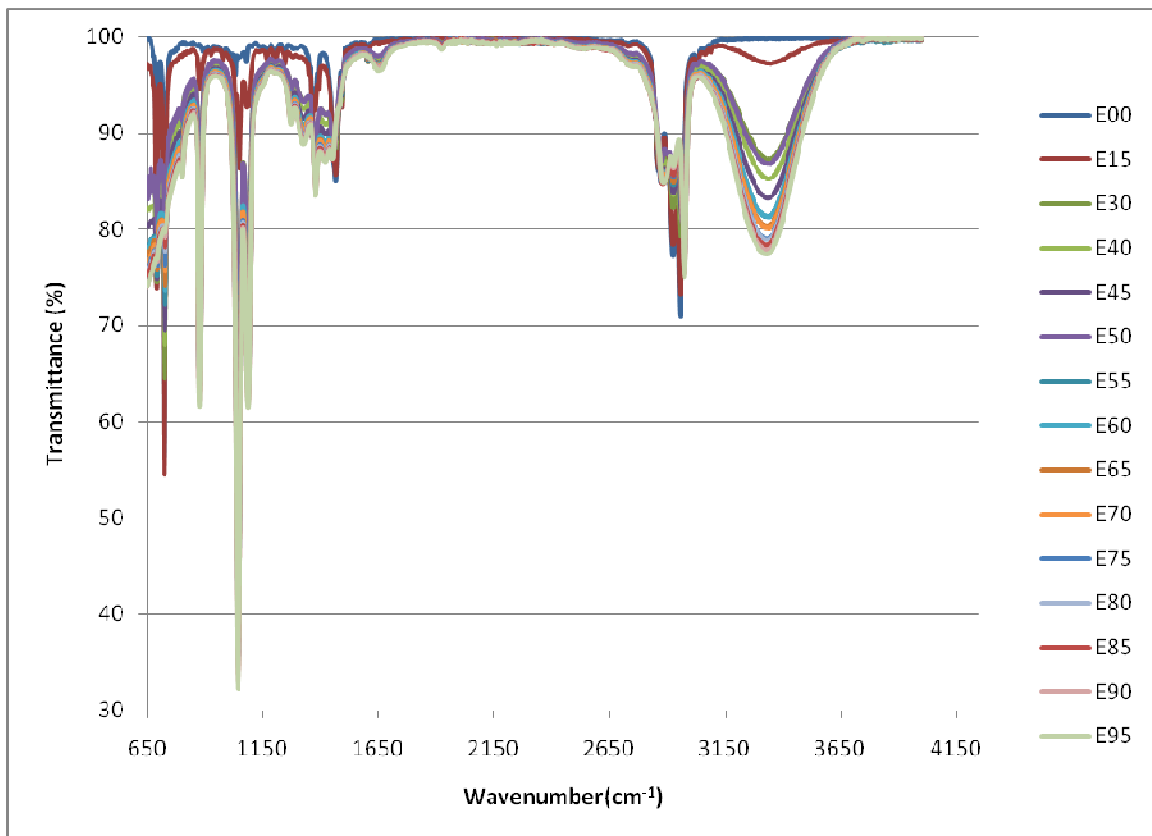


Figure 14. Infrared absorption for ethanol mixtures

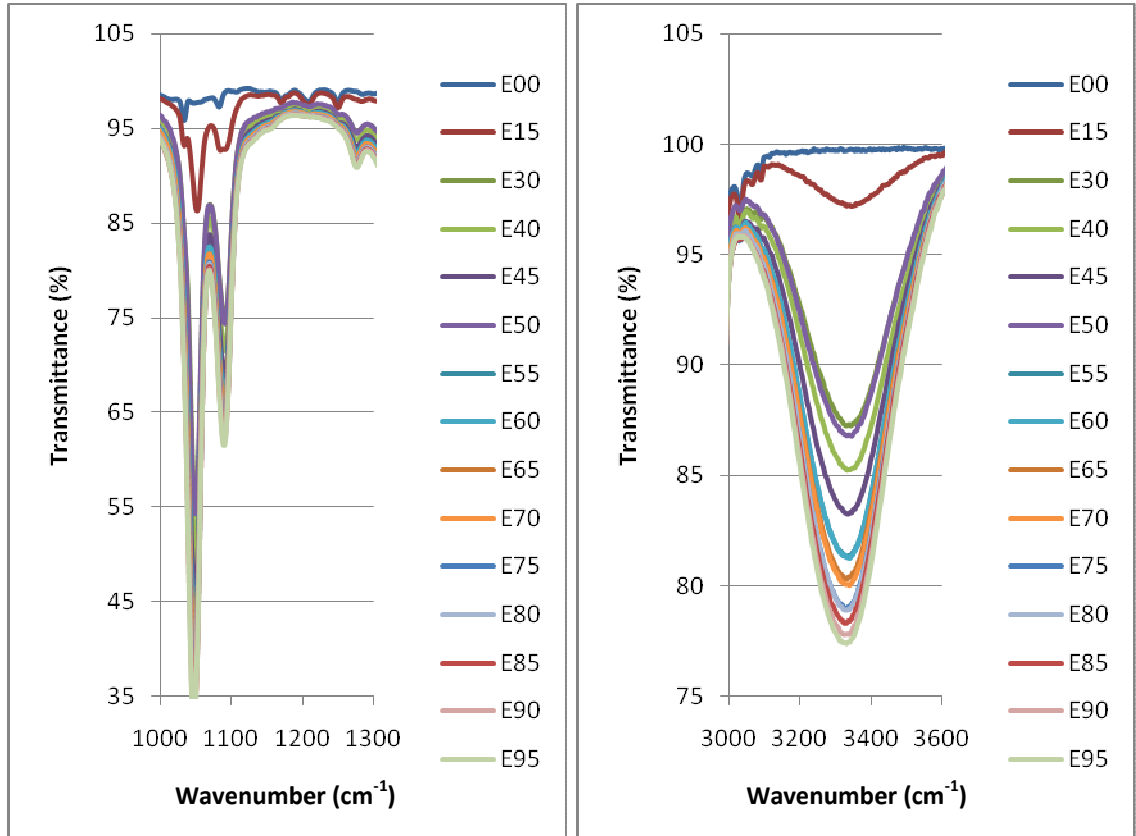


Figure 15. Infrared absorption for ethanol mixtures for OH and CO bonds

The incomplete mixing of ethanol and the MDA fuel renders the results from the E00 and E15 unreliable and are removed for trending. Additionally, it appears that the E50 mixture is flawed in that it does not follow the same trend as other mixtures and is also removed for analysis. As expected, the general trend in both the regions of interest is an increased adsorption as ethanol content increases. However, the correlation between ethanol content and infrared adsorption is not linear. A polynomial trend line is applied to the remaining data points and the resulting equations have an R-squared value above 0.99. Generally R-squared values near 1.00 are considered acceptable mathematical correlations.

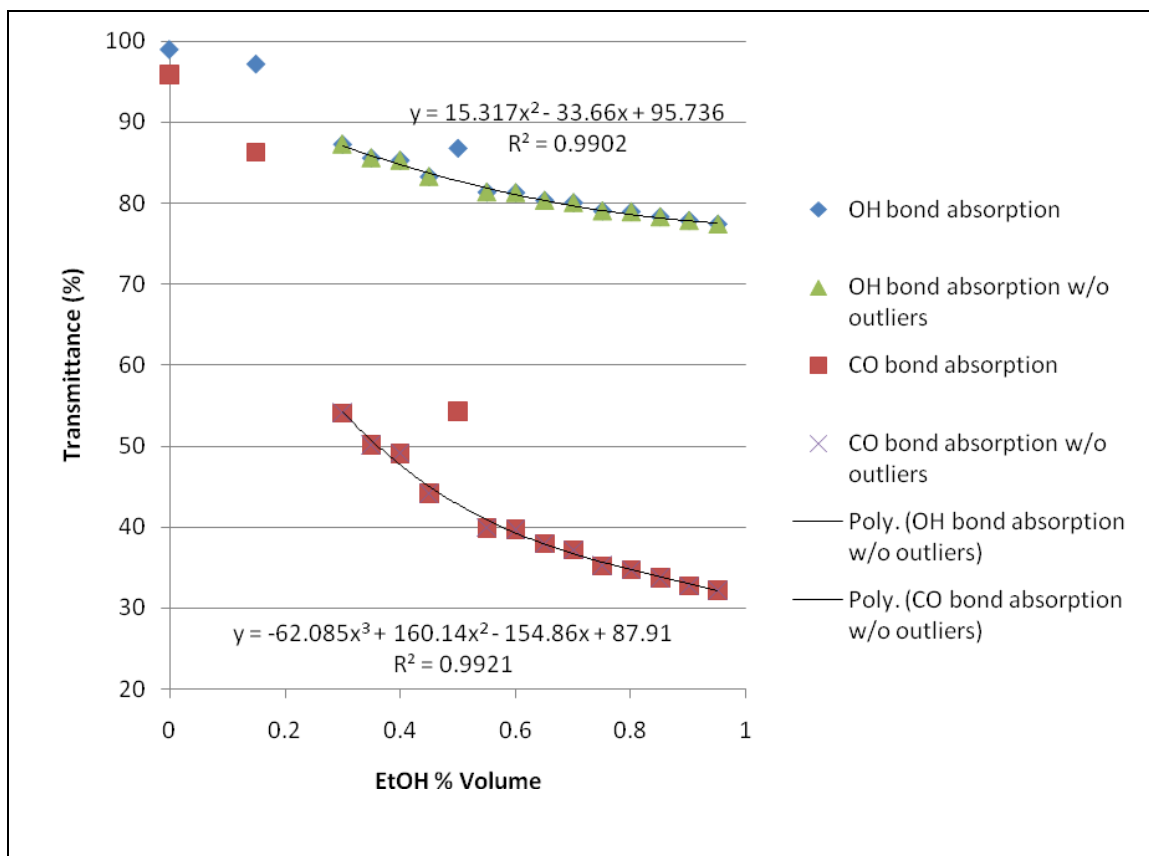


Figure 16. Infrared transmittance for ethanol mixtures

Based on the CO absorption data, the equation for ethanol content is

$$EtOH = -5X^3 * 10^{-5} + 7.5X^2 * 10^{-3} - 0.3974X + 7.6414 \quad (3)$$

where X is the minimum infrared absorption value within the CO band. Likewise, for the

OH bond the formula for ethanol content is

$$EtOH = 4.9Y^2 * 10^{-2} + 0.8641Y + 38.473 \quad (4)$$

where Y is the minimum infrared absorption value within the OH band. As a final method of comparison, a linear regression was performed using the absorption data from both the CO and OH infrared ranges. The equation developed from this analysis is

$$EtOH = 0.097X - 0.282Y + 19.673 \quad (5)$$

A comparison of these equations to the true ethanol content of the controlled samples is shown on Figure 17.

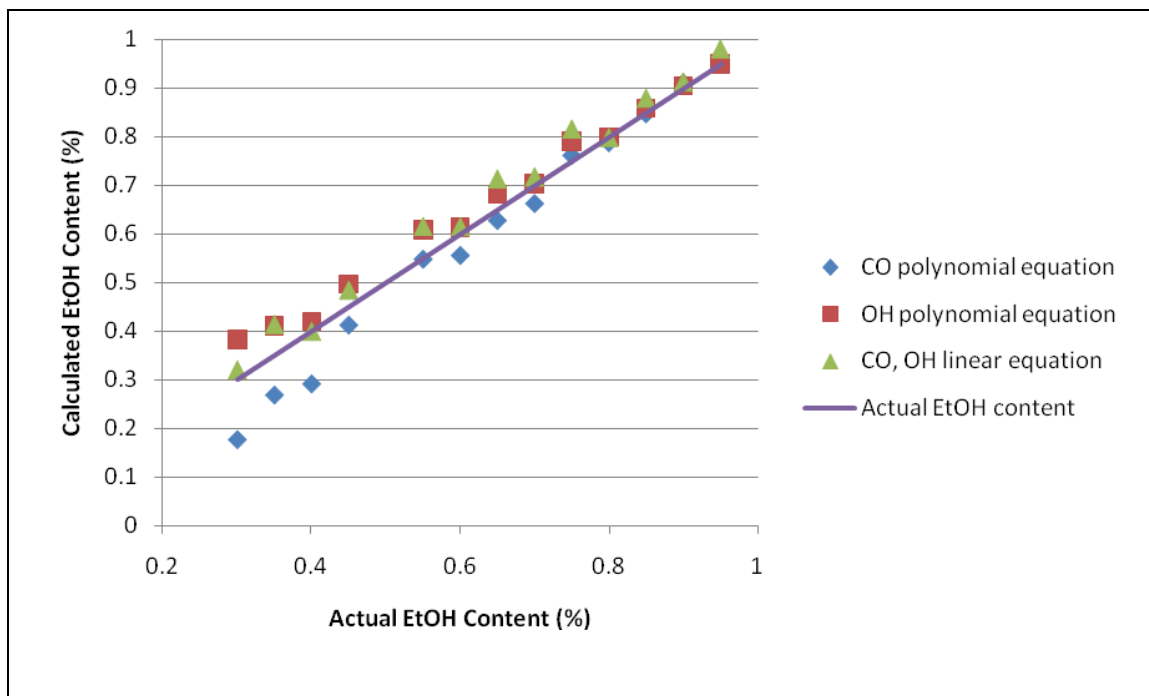


Figure 17. Ethanol content based on Infrared absorption

From these results it appears that IR absorption is a practical method of determining ethanol content for mixtures greater than 30% ethanol by volume. However, the AVUS system is designed to remove high concentrations of light hydrocarbons ($C < 6$) and only trace amounts of heavier hydrocarbons ($C \geq 7$). Therefore condensate samples are likely to contain less than 30% ethanol by volume. This phenomenon is complicated in that AVUS samples were stored in a freezer after being removed from the AVUS separator to prevent evaporation. As noted previously, ethanol solubility in MDA fuel decreases with temperature. When preparing the samples for chemical analysis, if two phases were present, each phase was removed and stored separately then individually analyzed. The lower, denser phase was labeled “H” for heavier, while the lighter phase

was labeled “L.” An example is the C-02 test which resulting in samples labeled C-02H and C-02L. Results from infrared analysis on these tests may be misleading.

Much of today’s consumer gasoline contains 0-10% ethanol by volume; therefore mixtures of these gasoline blends were not proven to be suited for IR detection by this study. For example, testing a sample of 87 octane Chevron gasoline for infrared absorption showed a transmittance of 96.6 for the OH bond and 82.5 for the CO bond. Based on this data and the equations from the preceding graph, one would expect a -5, 53, or 5% ethanol content based on the CO, OH, and linear equations respectively.

The spectrum results for the actual AVUS samples can be seen in Figure 18. As expected for AVUS condensates not taken from E85MDA fuel (A and B series tests), there is no transmittance in the regions of interest for alcohol content and are therefore not shown in Figure 18. However, the D series samples do display evidence of ethanol concentrations. The D-01 through D-R samples have decreased transmittance in the region indicative of the C-O bond. This decrease from one sample to the next suggests an increased ethanol concentration in each successive test. Based on the equations of ethanol content developed from the ethanol-MDA blends, ethanol content is calculated. These results are shown in Table 6 for the OH, CO and linear infrared transmittance equations. Samples from the C series test were not tested due to the limited volume of condensate produced from these tests.

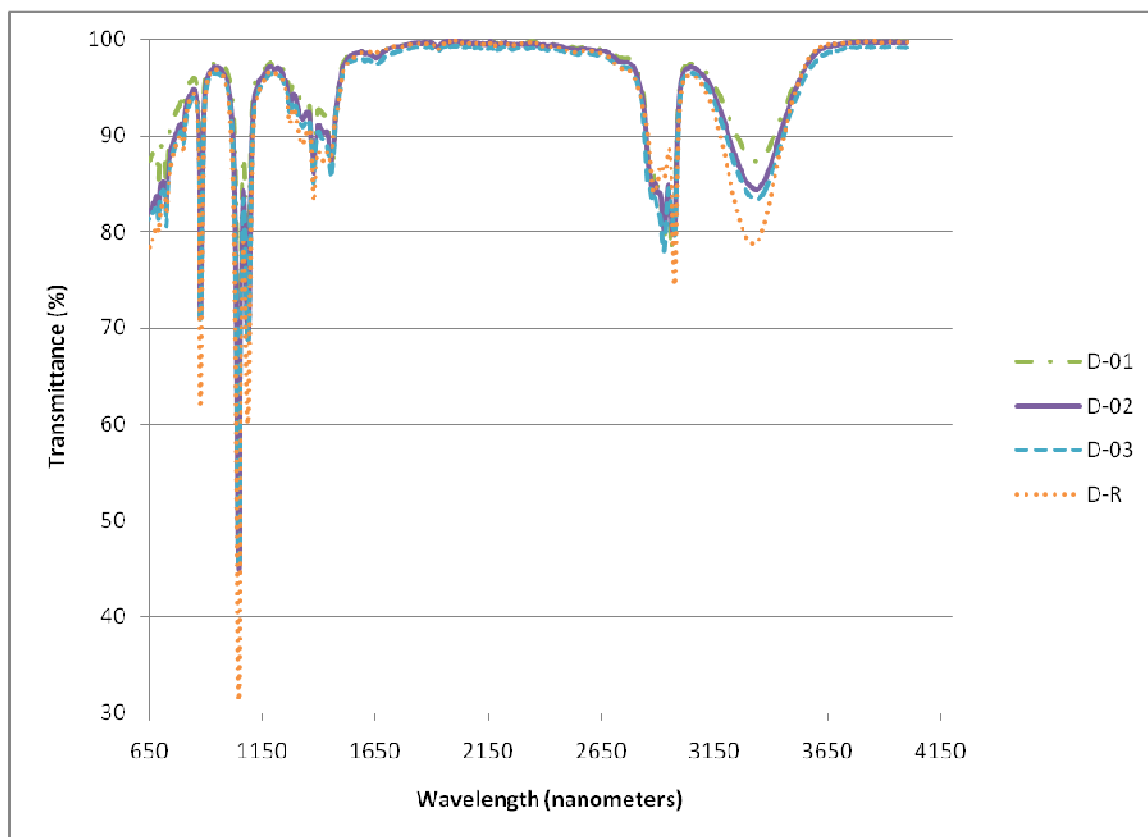


Figure 18. Infrared absorption for AVUS condensates

Table 6. Ethanol content based on infrared transmittance equations

Test	CO transmittance	OH transmittance	CO equation	OH equation	Linear equation	Actual EtOH%
D-01	57.98	87.32	6.7%	38.2%	67.4%	41%/8.9%
D-02	44.84	84.34	39.4%	45.0%	24.9%	N/A
D-03	45.11	83.36	38.7%	49.1%	54.0%	14.8%
D-R	31.28	78.66	101.9%	82.2%	52.6%	81.14%

As expected the results predict an increase in ethanol content for each successive test expect for the D-02 and D-03 results based on the C-O bond equation. However, due to the closeness of the C-O bond transmittance values for these tests the slight predicted decrease in ethanol content from D-02 to D-03 is acceptable. Of greater concern is the difference in the calculated ethanol values from the actual values. Due to various

circumstances such as the limited volume of the 300 series samples, the dual phases of the D-01 sample, and the D-02 sample that was not able to be analyzed, only 2 samples are available for comparison to the calculated results. From the data taken from the ethanol blends it appeared that the equation developed should have calculated the ethanol content within reason; however, none of the equations accurately predicted the ethanol content. The ethanol blends had a constant ratio of MDA hydrocarbon species while the AVUS condensates contained the same hydrocarbons in various concentrations. It is possible that molecular interactions with other hydrocarbon species affected the transmittance in the CO and OH ranges. More tests are needed to draw any conclusions from these equations and data. Future tests performed should investigate the area of the curve in specified regions as well as binary ethanol mixtures to analyze the effects of the various hydrocarbons on the measured spectrum.

Chemical Analysis Testing and Results

Previous AVUS samples were analyzed using the industry standard ASTM D6729 test which is capable of characterizing commercial gasoline by its individual components on a molar level by gas chromatography. However, the results of these tests proved inconclusive and expensive. Because of the MDA five component fuel used in this study, AVUS samples were analyzed more effectively by a simpler hydrocarbon analysis. Like the D6729, the test uses high resolution gas chromatography to characterize species by boiling point and carbon number; however the simplicity of the MDA fuel lessened the hydrocarbon possibilities significantly and decreases overhead costs allowing more samples to be tested. Detailed distillation curves were produced for the MDA and E85 MDA fuel while simulated distillation curves were produced for the actual AVUS

samples because of volume requirements. The laboratory required 150 mL samples for detailed distillation.

Dynalene Incorporated in Whitehall, PA performed all of the gas chromatography hydrocarbon analysis. Samples were sent to the laboratory using pairs of 5 mL vials labeled and coded by experiment run. To prevent leaks and breakage, special care was taken to ensure that the vials were tightly sealed and packaged in a padded absorbent material.

10 mL samples of the AVUS condensate and the residual fuel were tested for compositional analysis for two MDA major component fuel runs, and two E85MDA fuel runs. The results of these tests should have definitively shown the composition of the AVUS condensate and the AVUS residual fuel in comparison to the results predicted by the computer model for the first run on MDA fuel. For the E85MDA condensates, the infrared results will be used to compare actual ethanol content to that predicted by infrared absorption. Unfortunately, the results for many samples proved to be less than satisfactory with unknown percentages of the composition ranging from 2-37%. The composition of the parent fuels and the actual results broken down by carbon number on a percent volume basis can be seen on Table 7.

Table 7. Hydrocarbon composition of AVUS samples

	i-pentane	Hexane	Heptane	Toluene	i-octane	EtOH	Unknown
MDA	25	17.5	17.5	17.5	22.5	0	0
E85MDA	3.75	2.625	2.625	2.625	3.375	85	0
A-01	70.36	6.09	2.19	2.43	3.56	0	15.37
A-02	74.9	5.81	1.56	1.57	2.41	0	13.75
A-03	64.43	9.34	3.2	3.17	4.85	0	15.01
A-R	9.08	7.34	12.13	17.19	16.15	0	38.11
B-01	74.84	7.57	2.8	3.01	4.07	0	7.71
B-02	73.13	8.92	2.85	2.85	4.21	0	8.04
B-03	69.69	9.92	3.32	3.16	4.97	0	8.94
B-R	15.14	11.5	17.87	24.42	23.43	0	7.64
C-01	55.99	12.62	6.63	3.98	9.83	0.5	10.45
C-02H	33.24	7.59	3.8	2.36	5.63	38.65	8.73
C-02L	57.5	10.04	4.96	1.92	7.52	8.37	9.69
C-03	56.4	10.24	4.04	1.34	6.65	10.72	10.61
C-R	1.41	1.61	3.82	6.66	5.1	79.17	2.23
D-01H	24.35	5.98	4.02	2.04	6.08	40.45	17.08
D-01L	31.51	8.06	5.26	1.83	7.87	8.36	37.11
D-02							100
D-03	35.27	6.63	4.02	1.64	6.35	14.64	31.45
D-R	1.09	1.31	3.32	5.66	4.44	80.97	3.21

As the unknown percentage is less than 11%, B and C test series results will be used in the initial discussion of results for the MDA and E85MDA fuels respectively.

Furthermore, sample D-02 proved inconclusive as the lab had problems resolving baseline issues. As mentioned previously, A, B, C, and D denote the match of testing fuel while samples 01, 02, and 03 are taken from the first, second, and third sequential tests on the same batch of fuel. The R sample is taken from the residual fuel left in the fuel tank.

For the B series tests performed on the MDA fuel, there is a significant increase in iso-pentane in the AVUS condensate over the initial parent fuel. Even after repetitive tests on the same batch of fuel, the AVUS still produces starting fuel with at least 70% iso-pentane. However, it should be noted that though the concentration of light hydrocarbons remains high, the percentage of heavier species in the AVUS condensate increases slightly with each successive run. However, the residual fuel, sample B-R, shows a 10% drop in the concentration of iso-pentane. There is also a slight drop in the concentration of hexane, while the concentration of all the heavier components increases slightly. These results mean that the AVUS condensate would be an excellent starting fuel with over 70% light hydrocarbons; The fuel left in the fuel tank is slightly depleted of light hydrocarbons in comparison to the parent fuel; however, AVUS only removes vapors that would normally be removed by the carbon canister, so starting off of this parent fuel should not prove to be a problem.

The C series tests for the E85MDA fuel shows similar results with a 3.75-56% increase in the concentration of iso-pentane from the parent fuel to the condensate produced by the first run. Less than 1% ethanol is detected in this test. Results from most of the successive tests show similar results with iso-pentane concentrations over 55%. From this series of tests the only sample, other than the residual fuel, to have a lower iso-pentane concentration is C-02H. The original C-02 sample was collected from the second test run on this batch of E85MDA fuel; however, all of the samples were stored in a freezer to prevent evaporation. Unfortunately, the low temperatures had the effect of separating the sample into a denser, heavier (H) and a less dense, lighter (L) layer of hydrocarbons with unknown concentrations of species. It was thought that in colder

climates this separation could happen in the storage tank of an AVUS system and the various layers should be tested separately. The results show that this denser phase is more highly concentrated in ethanol than the top layer, but the concentration of iso-pentane in the denser phase has also increased and therefore proved to be a better starting fuel than the parent fuel. Furthermore, in any case where the fuel separated, the bottom layer composed less than a third of the total sample; however, exact volumetric measurements of the phases was not done.

The results of the residual fuel from the E85MDA tests show decreased concentrations of iso-pentane and hexane, while the concentrations of heptanes, toluene, and iso-octane actually increase. Surprisingly, the concentration of ethanol decreases as well. Because ethanol is the least volatile species of the mixture, the residual fuel actually increases in volatility and becomes a better starting fuel as well.

Although these results show that the AVUS produces an extremely volatile starting fuel, there are still up to 11% of the samples that are unknown. These unknown species could be either light or heavy hydrocarbons, or a combination of both. Worst case scenario would be to assume that the unknown species in the AVUS condensate were the least volatile species from the parent fuel. For the B series tests this would mean that the concentrations of toluene in the condensates would increase from around 3 to 11% and for the C series the volume of ethanol would increase to 11%, 47%, 18%, and 21%, for the C-01, C-02H, C-02L, and C-03 tests respectively. Even with this worse case assumption, the concentration of iso-pentane in each sample does not change and remains suitable for cold starts.

The data from a GC test is generally presented as a plot of the hydrocarbon detector response versus retention time. This provides a series of peaks at various times with each peak representing a different species present in the sample. The area under each of these peaks is proportional to the volumetric concentration of each component. Perhaps a better assumption would be to assume that each unknown species on the GC graph is the next known species that elutes from the sample. For example, unknown species that leave the distillation column after iso-pentane but before hexane would be assumed to be hexane. With this assumption, all of the unknowns are not lumped in with a single component but rather grouped with a known species that is of a similar volatility as the unknown species. With this assumption the only remaining unknown species are those that elute from the sample after toluene. This significantly reduces the amount of unknown species and simplifies the results. The results based on this assumption can be seen in Table 8.

This assumption increased the concentrations for many of the hydrocarbons at the expense of the unknown population of the tested samples. However, as the majority of the unknown species eluted from the test samples between the iso-pentane and hexane, the major effect of this assumption is an increased composition of hexane. The graphical results of this assumption are shown on Figures 19 and 20.

The results show that the AVUS produces a starting fuel with a very strong concentration of light hydrocarbons. The samples also have a fairly consistent composition run to run indicating the repeatability of the AVUS. The samples produced from the MDA fuel, tests A and B, have as much as 65% iso-pentane by volume and low concentrations of the heavier hydrocarbons such as heptanes, toluene, and iso-octane. A

fuel with a composition such as this would be an excellent starting fuel and has the potential to drastically reduce cold start emissions. The residual fuel, A-R and B-R, is not drastically changed from the parent fuel and should remain viable for cold start as AVUS only removes vapors normally captured by the carbon canister or lost to the atmosphere.

Table 8. Assumed hydrocarbon composition of AVUS samples

	i-pentane	Hexane	Heptane	Toluene	i-octane	EtOH	Unknown
MDA	25	17.5	17.5	17.5	22.5	0	0
E85MDA	3.75	2.625	2.625	2.625	3.375	85	0
A-01	70.78	19.49	2.19	2.43	5.12	0	0
A-02	75.52	17.47	1.57	1.58	3.87	0	0
A-03	64.58	21.84	3.2	3.17	7.22	0	0
A-R	22.08	11.39	12.13	17.22	37.04	0	0.137
B-01	75.21	12.98	2.8	3.01	6	0	0
B-02	73.4	14.43	2.85	2.85	6.48	0	0
B-03	69.97	15.96	3.32	3.23	7.53	0	0
B-R	15.16	15.85	17.87	24.43	26.7	0	0
C-01	55.99	19.94	6.63	3.98	12.83	0.62	0
C-02H	33.79	12.78	3.86	2.4	7.76	39.29	0.121
C-02L	57.54	17.04	4.99	1.92	9.92	8.49	0.09
C-03	56.48	18.15	4.05	1.39	9.03	10.85	0.113
C-R	1.41	3.28	3.82	6.66	5.61	79.21	0.014
D-01H	24.36	21.52	4.02	2.04	7.54	40.52	0.004
D-01L	32.45	41.36	5.42	1.89	9.94	8.85	0.078
D-02							100
D-03	35.4	36.13	4.03	1.64	7.95	14.79	0
D-R	1.1	3.89	3.33	5.67	4.88	81.14	0

The samples produced by AVUS from the E85MDA fuel is not as rich in light hydrocarbons as the MDA samples, yet are still volatile starting fuels. When compared to the E85MDA parent fuel, the AVUS fuels have as much as 50% iso-pentane by volume and less than 10% heptanes, toluene, and iso-octane in all but one case. In the cases

where the sample split into two phases, the results show that the more dense phases (D-01H and C-02H) have stronger concentrations of ethanol while their corresponding less dense phases (D-01L and C-02L) have less ethanol content. The samples that did not have dual phases generally had stronger iso-pentane concentrations. All the samples produced had an increased concentration of light hydrocarbons and therefore would be better starting fuels than the E85MDA.

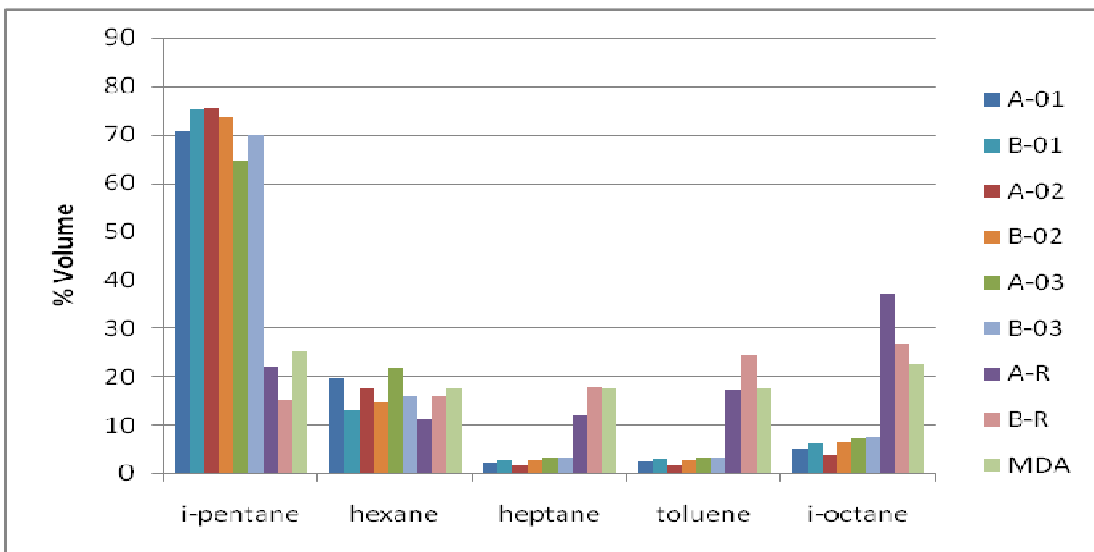


Figure 19. Assumed hydrocarbon composition of AVUS samples from MDA fuel

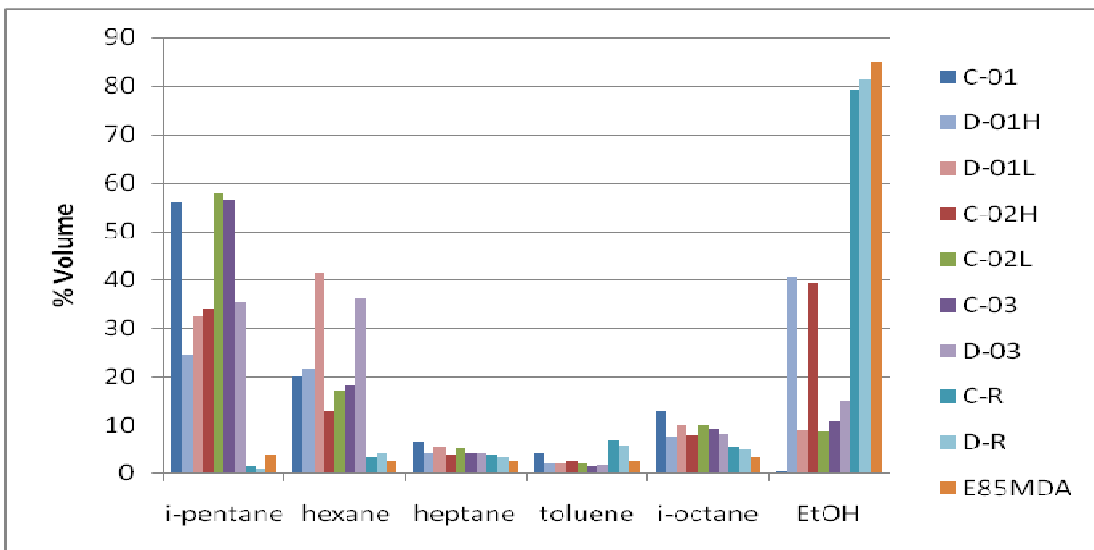


Figure 20. Assumed hydrocarbon composition of AVUS samples from E85-MDA fuel

The MDA and E85MDA parent fuels also underwent ASTM D86 volatility tests to produce distillation curves. Based on the results from the GC analysis, distillation curves were simulated for all of the AVUS condensate samples. Figure 21 shows the distillation curves of the AVUS condensate along with the parent fuels from which they were produced. The drivability indices (DI) for the same fuels are given in Table 9. DI is a common indication of fuel volatility and is given by $DI = 1.5T_{10} + 3T_{50} + T_{90}$. In this equation, T_N is the temperature at which N% of the fuel would be recovered based on the ASTM D86 and simulated distillation curves. Lower DI values are an indication of more volatile fuels as higher percentages of the fuel are recovered at lower temperatures (Standard Test, 2006).

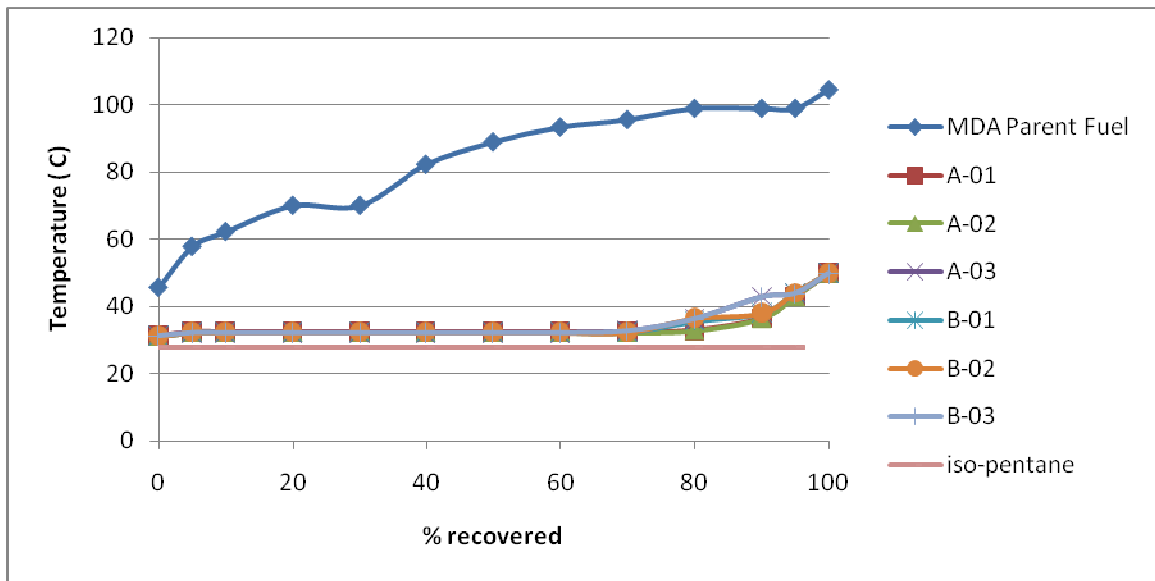


Figure 21. Distillation curves for AVUS samples from MDA fuel

Table 9. Drivability index of AVUS samples from MDA fuel

	MDA	A-01	A-02	A-03	B-01	B-02	B-03
T ₁₀	62.22	32.35	32.29	32.28	32.28	32.30	32.28
T ₅₀	88.89	32.35	32.29	32.28	32.28	32.30	32.28
T ₉₀	98.89	36.48	36.41	42.85	37.90	37.92	42.80
DI	458.89	182.04	181.70	188.11	183.17	183.27	188.04

Clearly observed from both the distillation curves and the drivability indices, the AVUS condensates are substantially more volatile than the MDA parent fuel from which it is produced. For example, T₉₀ for all of the condensate fuels is lower than the overpoint of the parent fuel. It should also be noted that the simulated curves for all 6 condensates tested are virtually identical, this indicates the repeatability of the AVUS on gasoline and the ability to produce more high volatile AVUS fuel from the same batch of gasoline. The relatively flat portion of the distillation curves indicates the large portion of the condensate that is iso-pentane. The graphs remain constant until 70% of the sample has been retrieved, consistent with the assumed 70% of the condensate being iso-pentane for the AVUS samples.

Similar results from the E85MDA fuel tests can be seen on Figure 22 and Table 10. As with the MDA fuel, the AVUS condensate is much more volatile than the parent fuel. Both the MDA and E85MDA condensates have DI values in the range of 181-190 with the values being slightly lower for the MDA condensates, as should be expected. However, the distillation curves for the E85 condensates are not as similar as the corresponding MDA fuel tests and the curve only remains constant through 50% recovery. These results are consistent with the 50% iso-pentane content.

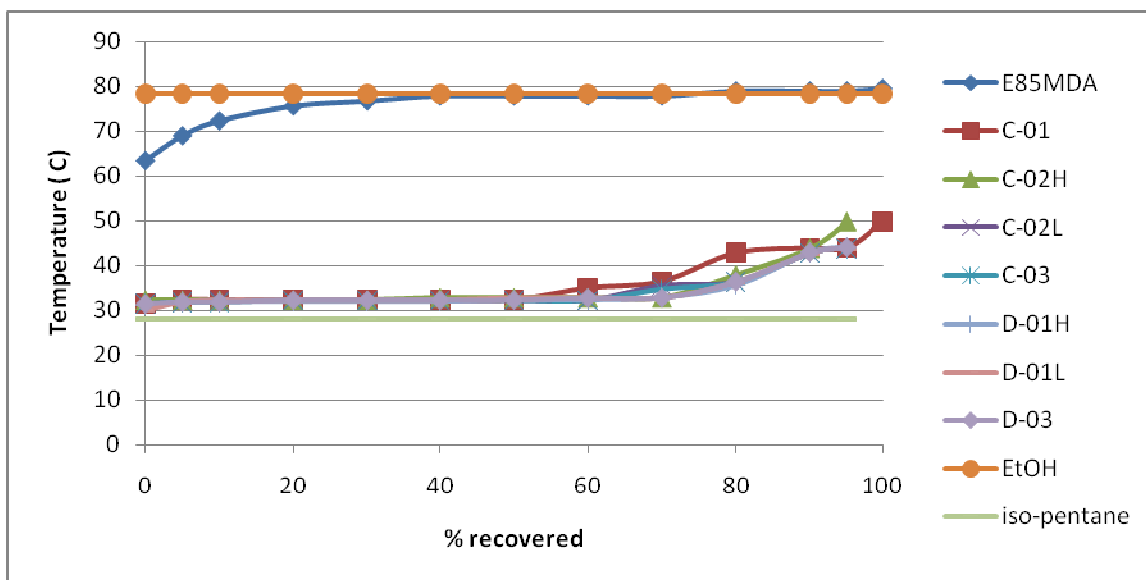


Figure 22. Distillation curves for AVUS samples from E85-MDA fuel

Table 10. Drivability index for AVUS samples from E85-MDA fuel

	E85-MDA	C-01	C-02H	C-02L	C-03	D-01H	D-01L	D-03
T_{10}	72.22	32.29	32.25	32.25	31.86	31.94	32.26	31.88
T_{50}	77.78	32.29	32.76	32.25	32.28	32.30	32.77	32.31
T_{90}	78.89	43.95	43.84	42.76	42.79	42.88	42.79	42.87
DI	420.56	189.25	190.48	187.89	187.42	187.70	189.50	187.61

As important as the composition of the AVUS condensates is the amount of condensate recovered from each test. Typical first runs on 2 L of MDA five component fuel produced nearly 80 mL of condensate while the second and third runs only produced around 30 and 10 mL, respectively. This decrease in condensate production can be attributed to the decrease in iso-pentane in the fuel tank. As the concentration of iso-pentane nears that of species in the mixture, vaporization slows and less condensate is produced in the same amount of time. It is likely that in a majority of the first runs, condensate vapors are collected in the separator in the earlier part of the test cycle before the boiling points of the other hydrocarbons species are reached. Though these vapors are

collected they do not condense until more of the nonvolatile species are removed from the separator and condensation is encouraged by high pressure.

However, the volumetric results from E85MDA fuel were much less. All runs on the ethanol fuel produced from 8-33 mL of AVUS starting fuel. The volumes captured for the E85MDA tests were consistently low. As the light species evaporate from the mixture, the concentration of overall hydrocarbon blend does not change significantly and therefore the amount of vapors leaving the fuel is not change radically either.

Comparing the E85MDA residual fuels to the parent fuel, it appears that over half of the iso-pentane is removed from the fuel tank. This, in combination with the low volumes of condensate formed, explains how the condensate can have iso-pentane concentrations from 35-55%. Considering that this amount of starting fuel was produced from only 2 L of parent fuel, it is likely that a 12 gallon fuel tank filled with E85 could produce over 340 mL of starting fuel from a single 90 minute AVUS run. The same tank filled with gasoline may produce 1.8 liters of starting fuel.

Table 11 shows the volumes of AVUS condensate and residual fuels collected for all four AVUS tests. Values given are the sum of the condensate collected immediately after the test and any condensate found in the system before the next test. Lost volumes are calculated values based on the tank beginning with 2 L of fuel. Lost volumes may be attributed to fuel remaining in the fuel tank and the AVUS; however, the overwhelming majority of the lost fuel is released to the atmosphere as non-condensable gases. All volumes are nominal values as a 100 mL graduated cylinder was used to do the measuring.

Table 11. Condensate and residual volumes collected

	Test A (MDA)	Test B (MDA)	Test C (E85MDA)	Test D (E85MDA)
1 st run (mL)	101	91	19	33
2 nd run (mL)	37	35	20	26
3 rd run (mL)	24	19	8	18
Residual (mL)	1630	1680	1820	1440
Lost (mL)	208	175	133	483

Chapter 6 AVUS COMPUTER MODEL

Introduction

NIST SUPERTRAPP program and MS Excel were used to model AVUS operation. SUPERTRAPP is program that predicts thermodynamic properties of pure fluids and fluid mixtures of up to 20 components. The FLASH routine was used to simulate both the AVUS fuel tank and separator. The inputs for FLASH are mixture composition, temperature, and pressure; the routine returns the phase fraction of liquid and vapor as well as the mole fraction of each component in each phase. The MDA five component fuel and nitrogen were used as the working fuels within the model. The temperature and pressure profiles used in the fuel tank portion of the model are based on an actual AVUS experiment; however, the separator portion of the model incorporates actual pressures but uses a constant temperature for simplification. A temperature correction factor was used to account for lower actual separator temperature. While this correction does change the number of moles in the condensate, it has little effect on the actual composition. The E85 mixture was not modeled because the NIST program does not contain thermodynamic properties for alcohols.

Assumptions

In order to simply the AVUS model many assumptions were made that are not characteristic of actual AVUS operation. To use the FLASH routine, it is assumed that the working fuels are all in liquid form and flashed at a specified temperature and

pressure. The resulting phase fractions and compositions are in equilibrium. However, in true AVUS operation, only the fuel is in liquid form and the nitrogen is a gas and the temperature and pressure within the fuel tank and separator are constantly changing – equilibrium is never realized. This is justified in that each iteration of the model represents only a fraction of a second and an equilibrium assumption is valid.

In actual AVUS operation, pressure release is achieved by removing vapors from either the fuel tank or the separator. The model mimics this by removing moles of species from the vapor fraction based on the ideal gas law. The ideal gas law is based on assumptions that the gas consists of a large number of molecules in random motion and obey Newton's laws of motion; the volume of the molecules is negligibly small compared to the volume occupied by the gas; and no forces act on the molecules except during elastic collisions of negligible duration. These assumptions are most valid at high temperatures and low pressures but have been used in this AVUS model as well. Because the majority of the vapor leaving the fuel tank is nitrogen, this assumption should cause minimum error. The pressure release also assumes that the vapor released is uniformly representative of the vapor phase of the flash. The model also assumes that these pressure releases are instantaneous and no new vapor is formed during the pressure release. In the next iteration of the model all unreleased vapor moles are added back to their respective liquid fractions and the process repeats.

No attempt is made to model energy losses within the AVUS apparatus. Experimental occurrences such as the compressor pressure release recirculation, system leaks, and liquid pooling within the system are not modeled. The model deals only with the thermodynamic interactions of the fuel at pressure release within the fuel tank and

separator. There are iterations within the separator portion of the model that do not represent a pressure release; these are modeled because the vapor addition from the fuel tank must be accounted for.

To convert the volumetric composition of the MDA five component fuel to molar values for the NIST program, accepted molar masses and densities were used. Later, these same values are used to convert the output values back to volumes. Also, the heptanes used in the experiments are a mixture of isomers; however n-heptane is used for the model. Table 13 shows the values used.

Table 12. Properties of MDA fuel component species at 25 °C and 100 kPa

	Density (g/cm ³)	Molar Mass (g/mol)
2-methylbutane	0.626	72.15
Hexane	0.655	86.18
Heptanes	0.684	100.21
Toluene	0.867	92.14
2,2,4-Trimethylpentane	0.688	114.11
Nitrogen	0.001251	28.0134

Fuel Tank

The fuel tank is the first section modeled. The model only accounts for times where there is a pressure release from the fuel tank because these are the only times when mass leaves the subsystem. For each iteration, the moles of each species, temperature, and pressure are entered into the SUPERTRAP FLASH routine. A pressure of 108.2 kPa (15.7 psia) is always used as the upper pressure limit for the AVUS fuel tank. The temperatures used are based on the temperatures seen at pressure release in an actual AVUS experiment. A screen capture from a sample iteration can be seen in Figure 23.

The number of moles of each species in each phase is determined by multiplying the mole fraction by the phase fraction and the moles of feed for each species. Based on the output from each iteration, the next feed composition is calculated by assuming only a fraction of the vapor leaves the subsystem. The equation used to do this is:

$$F_i = L_{i-1} + \frac{14.7}{15.7} * V_{i-1} \quad (6)$$

where F_i is the moles of feed of species i ; and L_{i-1} and V_{i-1} are the number of moles for the liquid and vapor phases of the previous iteration. The ratio of 14.7/15.7 is a result of the ideal gas equation used to determine the fraction of vapors that remain in the system.

Based on the ideal gas law:

$$\frac{P_1 V_1}{n_1 R T_1} = \frac{P_2 V_2}{n_2 R T_2} \quad (7)$$

Assuming that the temperature does not change during pressure release and volume remains constant, the equation becomes:

$$n_2 = \frac{P_2}{P_1} n_1 \quad (8)$$

Meaning that in order to relieve 6.9 kPa (1 psi) of pressure from the subsystem,

$(1 - \frac{P_2}{P_1})n_1$ moles have to be removed. The new feed mole values are then entered back into the FLASH routine and the process repeats. Several checks are used within the MS Excel program to ensure that correct values are entered. This process is repeated for 50 iterations.

```

Runs the NIST SUPPERTRAPP sof
298, 1.082

2-Phase Flash results at T = 298.000 K and P = 1.08200 bar

---Component----- --Feed---  --Liquid--  --Vapor---  ---Phi---  --K--
isopentane          0.271486    0.273666    0.230808    0.225814    .84E+00
n-hexane            0.166421    0.173504    0.342552E-01 0.333455E-01 .20E+00
n-heptane           0.149504    0.157038    0.890634E-02 0.863253E-02 .57E-01
toluene             0.206076    0.216517    0.112477E-01 0.109312E-01 .52E-01
2,2,4-trimethylpent 0.169792    0.178185    0.131646E-01 0.127402E-01 .74E-01
nitrogen            0.367219E-01 0.108921E-02 0.701618    0.703529    .64E+03
Molar Basis
                    1.00000    0.949135    0.500655E-01 Feed Fraction
                    88.3206    90.7659    42.6917    Molar Mass
                    0.560113E-01 0.569488E-02 0.794901    Comp. Factor, Z
                    0.777664    7.66829    0.438938E-01 D, mol/liter
                    -156.477    -162.425    -45.4931    H, kJ/mol
                    291.018    293.412    246.358    S, J/mol.K
                    180.175    186.670    58.9729    Cp, J/mol.K
                    1.30109    1.074.07    1.16883    Cp/Cv
                    1074.07    259.121    Sound Speed, m/s
                    -0.419202E-01 0.671582    JT, K/bar
                    3509.44    126.894    Visc., uP

```

Figure 23. Sample output from NIST FLASH routine

Fuel Tank Model Results

The purpose of this section of the model is to predict the final composition of the residual fuel after the vapors used to produce the AVUS condensate have been removed.

It is important that the AVUS does not significantly effect the composition of the fuel.

The original MDA fuel composition is seen on Table 14.

Table 13. Original MDA fuel composition

	% in MDA mixture	Vol in mixture (L)	Moles
2-methylbutane	25	0.50	4.34
Hexane	17.5	0.35	2.66
Heptanes	17.5	0.35	2.39
Toluene	17.5	0.35	3.29
2,2,4-Trimethylpentane	22.5	0.45	2.71
Nitrogen		13.14	0.59
Total		15.14	15.98

These mole values can be seen as mole fractions graphically here:

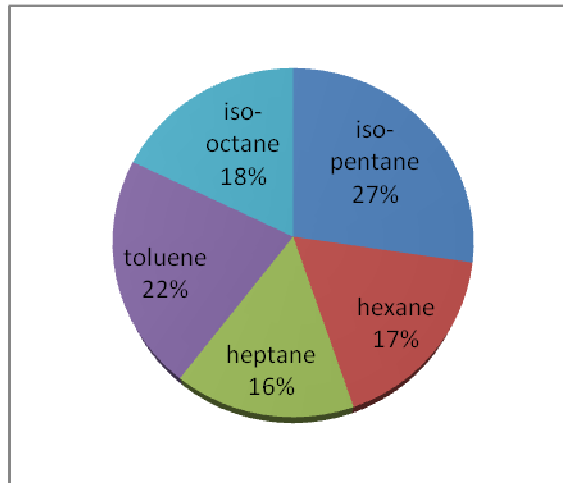


Figure 24. Initial fuel composition by mole percent

As expected, the number of moles of the various fuel species decreases over time as the temperature within the tank increases and pressure releases occur. The following graph shows the change in moles for each species for the 90 minute simulated experiment. It should be noted that though all the species experience a drop in moles, the most drastic change is seen in ic5, iso-pentane. This is also expected as iso-pentane is the most volatile of the MDA fuel components. The initial and final moles of each component can be seen on Table 15.

Table 14. Initial and final moles of MDA fuel components in computer model

	Iso-pentane	Hexane	Heptanes	Toluene	Iso-octane
Initial (mol)	4.34	2.66	2.39	3.29	2.71
Final (mol)	3.12	2.40	2.30	3.18	2.60

Based on the AVUS model, the initial and final percentage compositions of the fuel are shown side by side in Figure 25. Though the composition does change, it is not significant. The percentage of iso-pentane in the fuel decreases by 4%, but the

composition of each of the other components increases by 1% each. Figure 26 shows the change in temperature and moles of hydrocarbon species during the 90 minute test. This residual fuel should not pose a problem for normal vehicle operation, furthermore, this fuel should also be suitable for starts as the composition is not drastically low in volatile species. However, cold starts on this fuel would pose a greater emission problem as over fueling would have to be increased to compensate for the 4% of iso-pentane removed when compared to the parent fuel. Fortunately, the species are normally removed by the carbon canister and the residual fuel seen here should be similar to that found in vehicles currently.

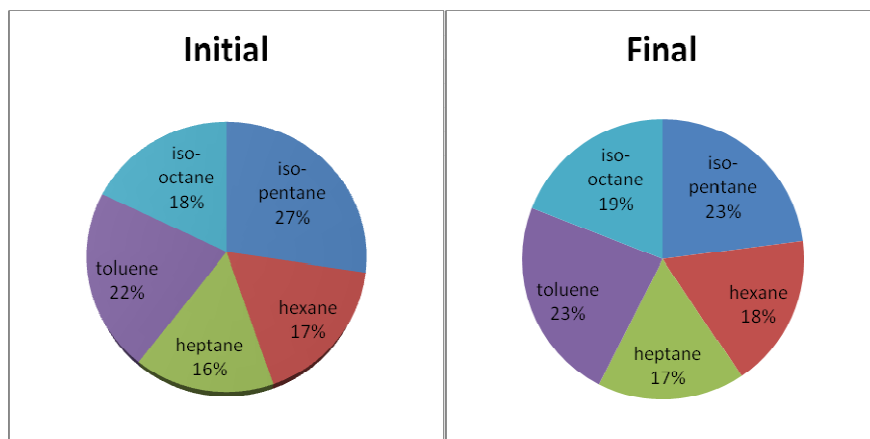


Figure 25. Initial and final fuel composition by mole percent

The AVUS model of the fuel tank also predicts the composition of the vapors that leave the fuel tank. Unexpectedly, there is a greater percentage of iso-pentane in the vapors that leave the fuel tank than nitrogen. However, nitrogen is not of any use as a starting fuel and is excluded from most analyses. The composition of the total exiting vapors represents the potential of the AVUS to produce a starting fuel if no useful vapors had to be released from the separator. Based on the MDA five component fuel, the condensate could be 69% light ends; however, commercial gasoline contains C2's

through C4's that will also be present in the condensate so there is potential for a starting fuel with 70% or more light ends. Unfortunately, some of the captured vapors must be released in order to keep the pressures within reasonable limits. The composition of the exit vapors can be seen on Figure 27.

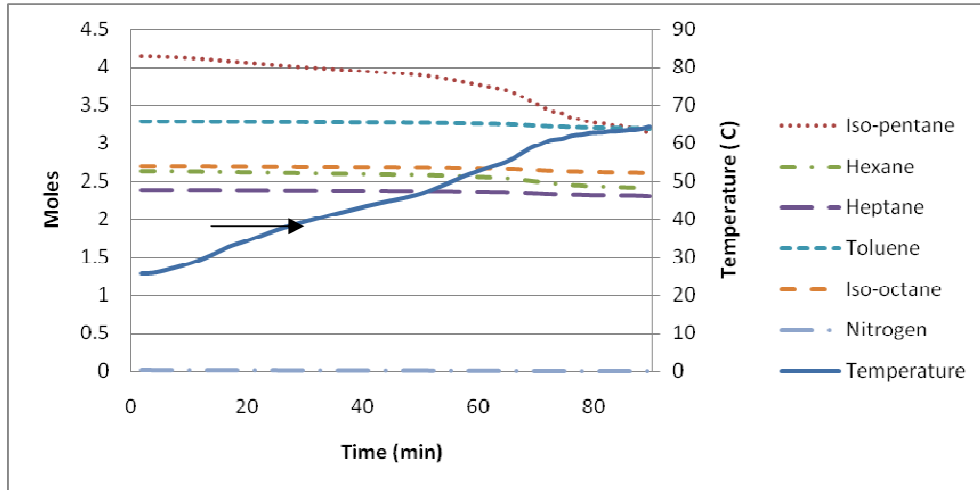


Figure 26. Change in fuel tank temperature and mole percentages

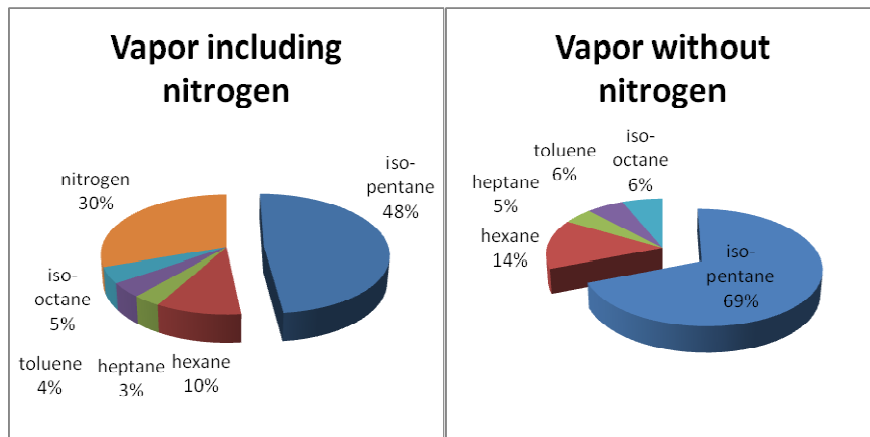


Figure 27. Total composition of the removed fuel tank vapors

Separator

Like the fuel tank model, the separator model only simulates the pressure releases events from the fuel tank as those are the only times mass entered the system. It also

assumes that the pressure release from the separator can only occur if the fuel tank releases pressure. For each event of the fuel tank, the mass released is added to the respective species mass already present in the separator. For fuel tank pressure release events where the separator does not release vapors, the extra mass from the fuel tank is still added to the separator but a flash calculation is not performed as no vapors are released. The iterations where separator pressure is, and is not, released is based on an actual AVUS experimental run.

For each iteration where pressure is released from the separator, the moles from fuel tank are added to the moles of each species already present in the separator. Then the total moles of each species, temperature, and pressure are entered into the SUPERTRAPP FLASH routine. A pressure of 690 kPa (100 psia) is always used as the upper pressure limit. Based on Alff's computer simulation, a constant temperature of 25 °C is used in the current AVUS model. Originally, the moles of each species used for feed input are given by the following equation:

$$F_{si} = L_{s,i-1} + \frac{1}{15.7} V_{i-1} + \frac{90}{100} V_{s,i-1} \quad (9)$$

where F_{si} is the moles of feed of separator species i ; $L_{s,i-1}$ and $V_{s,i-1}$ are number of moles for the liquid and vapor phases from the previous separator iteration. V_{i-1} is the portion of the fuel tank vapors released. The ratio of 90/100 is a result of the ideal gas equation used to determine the fraction of vapors that remain in the system.

For iterations after an event where pressure is not released from the separator, the moles from fuel tank are still added to the moles of each species already present in the separator yet a flash calculation is not performed for the current iteration since no mass

leaves the system as vapors during a pressure release. Therefore, the equation for feed calculation becomes

$$F_{s,i+1} = L_{s,i} + \frac{1}{15.7} V_i + V_{s,i} \quad (10)$$

since 100% of the vapors are used in the next feed calculation. As with the fuel tank model, the process is repeated for 50 iterations.

Separator Model Results

The purpose of this section of the model is to predict the final composition of the AVUS condensate. It is important that the AVUS does not significantly effect the composition of the fuel while producing a starting fuel capable of low emission cold starts. This should be easily accomplished as AVUS only removes those vapors which would have normally been captured by the vapor canister. As the temperature within the fuel tank increases and vapors are released to the separator, hydrocarbon species are collected and condensed. This AVUS model predicts the final composition of the starting fuel, as well as the moles of each species lost as vapor. The predicted condensate can be seen on Figure 28. The final FLASH calculation is performed at a pressure of 101 kPa because the sampling pressure is atmospheric. A starting fuel with 62% iso-pentane is more than capable of starting a vehicle at even the most severe cold temperature.

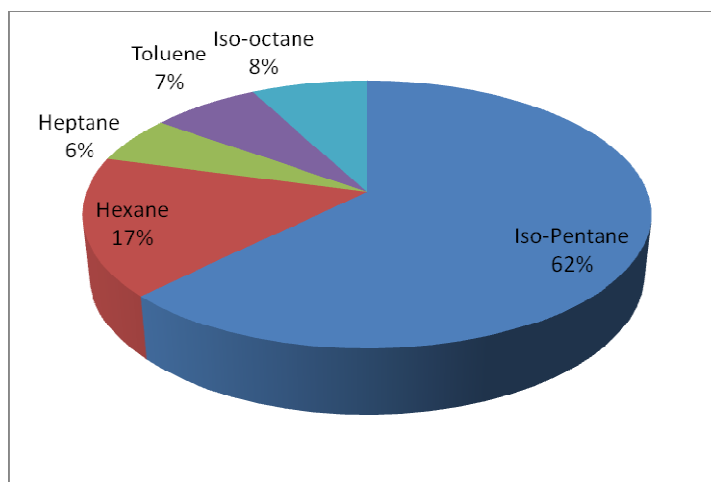


Figure 28. AVUS model condensate composition

Almost as important as the composition of the condensate is the amount of condensate produced. The model, as well as the actual experiments, starts with 2 L of MDA fuel with the composition shown in Table 16. The model predicts the final composition of both the residual fuel and the condensate; based on the law of conservation of mass the amount of fuel lost as vapors from the separator can also be predicted. These values are shown Table 16.

Table 15. Model composition of both the residual fuel and the condensate fuel

	Iso-pentane	Hexane	Heptanes	Toluene	Iso-octane	Total
Fuel (mol)	4.34	2.66	2.39	3.29	2.71	15.39
AVUS Fuel (mol)	0.630	0.168	0.058	0.073	0.078	1.008
Residual (mol)	3.12	2.40	2.30	3.18	2.60	13.61
Lost (mol)	0.584	0.091	0.028	0.035	0.038	0.775
Vol Fuel (mL)	500.00	350.00	350.00	350.00	450.00	2000.0
Vol AVUS Fuel(mL)	72.71	22.17	8.53	7.76	12.97	124.14
Vol Residual (mL)	360.02	315.79	337.35	338.50	430.73	1782.4
Vol Lost (mL)	67.27	12.04	4.12	3.74	6.29	93.46

Starting with 2 L of MDA five component fuel, the model predicts that AVUS should produce 124 mL of a 61% iso-pentane starting fuel while leaving almost 1800 mL of a residual fuel capable of running a vehicle for normal operation. However, the model also predicts that almost as much iso-pentane is lost to the carbon canister as is saved in the AVUS condensate. The AVUS saves just over half of the vapors produced in the fuel tank. This represents over a 50% reduction of vapors that are lost to the carbon canister in a non-AVUS vehicle under similar conditions.

Separator Temperature Correction and Results

After reviewing the results and assumptions, it was realized that a constant separator temperature of 25 °C is not a justified assumption and that a temperature of 40 °C is more justified based on actual AVUS separator temperature profiles. To correct this error within the AVUS separator model, the ideal gas law is used to calculate a correction factor.

$$n_2 = \frac{P_2 T_1}{P_1 T_2} n_1 \quad (11)$$

Therefore the new feed equation becomes

$$F_{s1} = L_{s,t-1} + \frac{1}{15.7} V_{t-1} + \frac{90}{100} * \frac{298}{313} V_{s,t-1} \quad (12)$$

The correction factor does not take into account the change in phase and equilibrium composition in the FLASH calculations, but because of the small temperature difference the resulting error was minimal. The model composition based on the correct factor is seen here in Figure 29.

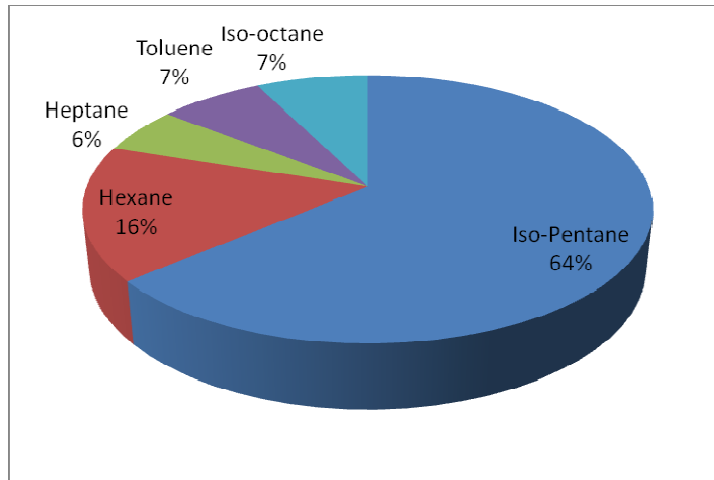


Figure 29. AVUS condensate composition with temperature correction

The correction factor has the effect of slightly increasing the percent of iso-pentane by 2% while decreasing the amount of both iso-octane and hexane by 1% each. The actual composition of the AVUS condensate does not change drastically, but there is an effect on the volumes of condensate saved and vapors lost as seen in Table 17. The increased separator temperature has the effect of increasing the vapors lost to the carbon canister and decreasing the amount of condensate produced. The volume of condensate is reduced by 10 mL that shows up in vapors lost. This is a notable trend. As separator temperature increases, condensate decreases. In experiments, efforts should be made to keep the separator temperature low so that more of the valuable fuels condense for a starting the fuel.

Table 16. Final composition of both the residual fuel and the condensate fuel with temperature correction

	Iso-pentane	Hexane	Heptanes	Toluene	Iso-octane	Total
Fuel (mol)	4.34	2.66	2.39	3.29	2.71	15.39
AVUS Fuel (mol)	0.576	0.154	0.053	0.067	0.072	0.924
Residual (mol)	3.12	2.40	2.30	3.18	2.60	13.61
Lost (mol)	0.637	0.106	0.033	0.041	0.045	0.860
Vol Fuel (mL)	500.00	350.00	350.00	350.00	450.00	2000.0
Vol AVUS Fuel(mL)	66.57	20.30	7.81	7.11	11.88	113.66
Vol Residual (mL)	360.02	315.79	337.35	338.50	430.73	1782.4
Vol Lost (mL)	73.40	13.91	4.84	4.39	7.39	103.93

The AVUS model presented in Table 17 predicts an initial AVUS run on MDA fuel would produce 114 mL of starting fuel that is 64% iso-pentane by volume. Actual AVUS tests produced 101 mL of a 71% iso-pentane fuel and 91 mL of a 75% iso-pentane fuel for the A and B series tests respectively. The model's accuracy in comparison to the actual AVUS fuel is shown in Table 18. However, the model under predicted the concentrations of iso-pentane and hexane while over predicting the concentrations of iso-heptane, toluene, and iso-octane.

Table 17. Comparison of model and actual AVUS results

	Iso-pentane	Hexane	Heptane	Toluene	Iso-octane
Model	64	16	6	7	7
A-01	70.78	19.49	2.19	2.43	5.12
B-01	75.21	12.98	2.8	3.01	6.00

AVUS Model Considerations

As mentioned previously, the model makes no attempt to completely model the entire AVUS. Both the fuel tank and separator models simulate only the pressure release events where mass is exchanged between the fuel tank, separator, and carbon canister. Therefore there are experimental considerations that will make the ideal model results different from the actual results from AVUS experiments.

The model assumes that the vapor released from both the fuel tank and separator is completely uniform. In the AVUS separator, the pressure released is located near the inlet from the compressor and the pressure within the separator is only release while the compressor is running. Therefore when the pressure valve in the separator is opened is likely that a high concentration of fuel vapor is released before any species have been able to be condensed. This will result in higher than expected vapor losses and low condensate volumes.

There are also many places within the AVUS where condensate may form and pool. This liquid may remain in the system and not flow to the separator for collection. This also results in low condensate volumes. The actual AVUS has a vapor recirculation loop to relieve pressure downstream of the compressor after compressor operation. This means that species mass is added back to the fuel tank. The AVUS model does not take this into account; however, the volume of vapor returned to the fuel is small so minimum error resulted.

Chapter 7 CONCLUSIONS AND RECOMMENDATIONS

Introduction

It is obvious from the chemical analysis results that the AVUS is very capable of producing a starting fuel with a significant concentration of light hydrocarbons. The AVUS successfully collected, condensed, and stored fuel vapors for later use in cold starts. By collecting evaporative emissions from a fuel tank, a system such as AVUS could help to reduce evaporative and cold start emissions. This study aimed to simplify the work done by Alff and Ashford and go a step further examine inexpensive methods of determining the condensate composition.

Conclusions

The following points summarize the major conclusions of this study:

- AVUS is very capable of producing a starting fuel from the vapors produced in a fuel tank during normal operation. If used on a gasoline powered vehicle, the AVUS would reduce the volume of hydrocarbons collected in the carbon canister by converting them into a volatile starting fuel
- The AVUS is capable of producing a starting fuel from E85 vapors. The fuel produced has a higher concentration of light hydrocarbons than the parent fuel and therefore better for cold starts. However, the quantity of starting fuel produced is much less than that from the same volume of non-alcohol fuels.

- Successive AVUS tests on the same batch of MDA major component and E85MDA fuels prove that the system can repetitively produce a volatile starting fuel, without depleting the parent fuel of hydrocarbon species needed for regular cold starts
- While index of refraction can be used as a relative indicator of hydrocarbon composition, it is not suitable as an absolute indication of the species makeup of a fuel. AVUS fuel, a gasoline derivative, is made up from many hydrocarbons with various indices of refraction; therefore an infinite combination of the five components of the MDA fuel can result in any index of refraction value
- There is great potential for infrared transmittance measuring for the determination of ethanol content in fuels. The strength of the infrared absorption in the ranges near $3600\text{-}3000\text{ cm}^{-1}$ and $1300\text{-}1000\text{ cm}^{-1}$ of particular interest due to the OH and CO bonds found only in alcohols. The infrared absorption in these ranges could be used to determine alcohol content.
- The Ashford (2003) OBDS produced a starting fuel composed of nearly 50% light ends. This fuel was able to reduce catalyst light off time by >50%, hydrocarbon emissions by > 50% and CO emissions > 65% respectively. In comparison to starting fuels produced in these studies, it can be assumed that a significant reduction in cold start emissions will occur if an AVUS fuel composed of more than 65% light ends is used.

Recommendations

For future AVUS research the following items are recommended:

- Both evaporative emission (SHED testing) and tailpipe emissions (FTP testing) on vehicle testing
- More in depth look at infrared absorption as a method of determining ethanol content in gasoline
- When testing AVUS samples, also send standards and parent fuels for GC testing

REFERENCES

- Air Quality Index (AQI) - A Guide to Air Quality and Your Health*. Retrieved August 10, 2008, from <http://airnow.gov/index.cfm?action=static.aqi>
- Alff, M., *Experimental Study of an Active Vapor Utilization System for Use in Gasoline Powered Vehicles*, Thesis, The University of Alabama, 2007.
- Ashford, M., Matthews, R., Hall, M., Kiehne, T., Dai, W., & Curtis, E. (2003). *An on-board distillation system to reduce cold-start hydrocarbon emissions*. SAE paper 2003-01-3239.
- Ashford, M., & Matthews, R. (2005). *Further development of an on-board distillation system for generating a highly volatile cold-start fuel*. SAE paper 2005-01-0233.
- Ashford, M., & Matthews, R. (2006). On-Board Generation of a Highly Volatile Starting Fuel to Reduce Automobile Cold-Start Emissions. *Environmental Science and Technology*, 40, 5770-5777.
- Brochert, A. (November 3, 2000). *Smog-Related Health Problems*. Retrieved August 10, 2008, from http://www.personalmd.com/news/smogrelated_1103000.shtml
- Brocos, P., Pineiro, A., Bravo, R., & Amigo, A. (2003). Refractive Indices, Molar Volumes and Molar Refractions of Binary Liquid Mixtures: Concepts and Correlations. *Phys. Chem. Chem. Phys.*, 5, 550-557.
- Buell, Phyllis & Girard, James. (2003). *Chemistry Fundamentals: An Environmental Perspective*. Sudbury, MA: Jones and Bartlett Publishers.
- Chen, H., & Tu, C. (2005). Densities, Viscosities, and Refractive Indices for Binary and Ternary Mixtures of Acetone, Ethanol, and 2,2,4-Trimethylpentane. *Journal of Chemical and Engineering Data*, 50(4), 12162-1269.
- Commonly Asked Questions about ORVR*. Retrieved September 26, 2006, from <http://www.epa.gov/otaq/regs/ldhwy/onboard/orvrq-a.txt>
- El-Sharkawy, A. E., Jeffers, J., "Transient Fuel System Thermal and Emissions Analysis," SAE 980049.
- Falate, R., Muller, M., Fabris, J. L., Kalinowski, H. J. (2003). Long Period Grating in Standard Telecommunication Optical Fibers for Fuel Quality Control. *Annals of Optics*, 5.

- Gumus, M. (2008). Reducing cold-start emission from internal combustion engines by means of thermal energy storage system. *Applied Thermal Engineering*. doi:10.1016/j.applthermaleng.2008.03.044
- History*. Retrieved August 10, 2008, from <http://www.epa.gov/history/>
- Karknis, A.N., Botsaris, P.N., & Sparis, P.D. (2004). Emission reduction during cold-starts via catalyst surface control. *Proceedings of the Institution of Mechanical Engineers, Part D: Journal of Automobile Engineering* 218, 1333-1340.
- Lebowitz, J., Lovette, J., Chan, C., & Frich, D. (2005). *Activated carbon coated polymeric foam for hydrocarbon vapor adsorption*. SAE paper 2005-01-1103.
- Li, G., Li, L., & Qiu, D. (2006). The Study of the Control on The First Firing Cycle for Reducing the Cold Start Emissions in a Liquid Petrol Gas Spark Ignition Engine. *IEEE*. 485-90.
- Lyons, J., Lee, J., Heirigs, P., McClement, D., & Welstand, S. (2000). *Evaporative emissions from late model in-use vehicles*. SAE paper 2000-01-2958.
- Na, K., Kim Y. P., Moon, I., & Moon K. (2004). Chemical Composition of Major VOC emission sources in the Seoul Atmosphere. *Chemosphere*, 55, 585-594.
- Ramanathan, K., West, D.H., & Balakotaiah V. (2004). Optimal design of catalytic converters for minimizing cold-start emissions. *Catalysis Today*. 357-373.
- Reddy, S. (2004). U.S. Patent No. 6,769,418. Washington, DC.: U.S. Patent and Trademark Office.
- Reusch, William. (1999). Infrared Spectroscopy. In *Spectroscopy*. Retrieved September 21, 2008, from <http://www.cem.msu.edu/~reusch/VirtualText/Spectrpy/spectro.htm#contnt>
- Santoso, H., & Cheng, W. K. (2002). *Mixture Preparation and Hydrocarbon Emissions Behaviors in the First Cycle of SI Engine Cranking*. SAE paper 2002-01-2805.
- Seader, J. D., and Henley, E. J. (2008). *Separation Process Principles*. New York: John Wiley & Sons, Inc.
- Senda, J., Higaki, T., Sagane, Y., & Fujimoto, H. (2000). *Modeling and Measurement on Evaporative Process of Multicomponent Fuels*. SAE paper 2000-01-0280.
- Servati, H., Marshall, S., Murphy, J., Sanei, M., Zhou, W., & Lewis, W. (2005). *Carbon canister-based vapor management system to reduce cold-start hydrocarbon emissions*. SAE paper 2005-01-3866.

Standard Test Method for Distillation of Petroleum Products at Atmospheric Pressure, ASTM D86; ASTM International: West Conoshockton, PA, 2006.

Taylor, J., & Van Doren, P. (2006). Gasoline Prices in Perspective. *Investor's Business Daily*.

Technology Transfer Network National Ambient Air Quality Standards (NAAQS). Retrieved August 10, 2008, from <http://www.epa.gov/ttn/naaqs/>

The South Coast Air Quality Management District (AQMD). Retrieved August 10, 2008, from <http://www.aqmd.gov/Default.htm>

Tier 2 Vehicle & Gasoline Sulfur Program. Retrieved August 10, 2008, from <http://www.epa.gov/otaq/regs/ld-hwy/tier-2/>

Appendix A: Data Results from Parent Fuels and AVUS Samples

	T _{avg fuel} (°C)	P _{avg tank} (kPa)	P _{avg sep} (kPa)	Vol (mL)	Avg Index of Refraction	OH transmittance	CO transmittance		% ic5	% c6	% c7	% toluene	% ic8	% EtOH	% Unknown species	Drivability index
MDA					1.4007				25	17.5	17.5	17.5	22.5	0	0	458.89
E85MDA					1.3683				3.75	2.625	2.625	2.625	3.375	85	0	420.56
Model									64	16	6	7	7	0	0	
A-01	46.51	4.32	501.94	101	1.3698	99.52	97.59		70.78	19.49	2.19	2.43	5.12	0	0	182.04
A-02	50.4	4.06	405.07	37	1.3788	99.41	96.88		75.52	17.47	1.57	1.58	3.87	0	0	181.70
A-03	48.15	4.05	414.31	24	1.3822	99.40	96.03		64.58	21.84	3.2	3.17	7.22	0	0	188.11
A-R				1630	1.4077	99.46	95.97		22.08	11.39	12.13	17.22	37.04	0	0.137	
B-01	45.59	4.59	635.83	91	1.3752	99.55	97.56		75.21	12.98	2.8	3.01	6	0	0	183.17
B-02	50.7	3.75	433.20	35	1.3745	99.60	98.52		73.4	14.43	2.85	2.85	6.48	0	0	183.27
B-03	49.06	4.01	435.40	19	1.3794	99.51	96.85		69.97	15.96	3.32	3.23	7.53	0	0	188.04
B-R				1680	1.4107	99.52	96.05		15.16	15.85	17.87	24.43	26.7	0	0	
C-01	49.05	4.14	653.83	19					55.99	19.94	6.63	3.98	12.83	0.62	0	189.25
C-02	48.15	4.14	612.74	20				H	33.79	12.78	3.86	2.4	7.76	39.29	0.121	190.48
								L	57.54	17.04	4.99	1.92	9.92	8.49	0.09	187.89
C-03	47.32	3.87	629.08	8					56.48	18.15	4.05	1.39	9.03	10.85	0.113	187.42
C-R				1820					1.41	3.28	3.82	6.66	5.61	79.21	0.014	
D-01	46.61	4.07	581.57	33	1.3716	87.32	57.98	H	24.36	21.52	4.02	2.04	7.54	40.52	0.004	187.70
								L	32.45	41.36	5.42	1.89	9.94	8.85	0.078	189.50
D-02	47.06	3.94	640.52	26	1.3755	84.34	44.84								100	
D-03	47.41	3.59	625.56	18	1.3763	83.36	45.11		35.4	36.13	4.03	1.64	7.95	14.79	0	187.61
D-R				1440	1.3664	78.66	31.28		1.1	3.89	3.33	5.67	4.88	81.14	0	

